Reply to Referee #1 (Dr Dongkyun Kim)

We thank Dr Dongkyun Kim for his careful reading of the paper and his perceptive comments.

Here are responses to the points made by Dr Kim.

(1) Dr Kim first points out that the model equations suggest that, when parameter α is reduced, the tail of the distribution of cell intensities becomes thinner, which will reduce the estimates of extreme values for given return periods. This in turn should therefore

improve the model's fitting ability to rainfall characteristics with "more regular" behavior.

Ans: First, we would like to point out that the variance of η is rather: $Var(\eta) = \frac{\alpha}{\nu^2}$. This does not, however impact the point made by the referee, which is an interesting one: if α is smaller, the variance of the distribution of the mean cell intensity in a storm, namely μ_X, is decreased, and this Gamma distribution will therefore have a thinner tail. This might indeed mean that the model is better designed to reproduce the 'regular behaviour' of rainfall.

This would also however seem to imply that it performs less well in terms of extremes, which is not the case. I think that it is probably difficult to draw conclusions insofar as the value of parameter ν also changes with the value of α.

(2) Dr Kim, who has access to the same data set we used in the paper, points to an apparent discrepancy in the observed annual maxima.

The observed annual maxima shown in Figure 11 and Figure 12 seems to be lower than the actual value. According to my calculation, the observed annual maximum of daily rainfall goes upto 90+ mm while the values shown in the figure goes upto only 70mm. I guess this discrepancy came from the way to estimate the annual maxima. In my case, I ran the moving window of a given aggregation interval throughout the 5-minute timeseries over one year to get the maximum value, while the authors aggregated first and then took the maximum

Ans: As the referee indicates, this discrepancy is due to the fact that we have considered daily maxima, while he has been working with 24-hour (moving-window) maxima. We chose not to use moving-window aggregation in order to be consistent with that in Kaczmarska et al. (2014), where the same Bochum dataset was used (see Figure 8 in Kaczmarska et al. (2014)). It is interesting though to note the discrepancy that is obtained, and in principle, we could also include a figure in which we compare the 24-hour extremes from observations and model simulations. Given the fact that the paper is already rather long, and that some additional material will need to be included to address other referee comments, we opt for not including this. In so doing, we are following standard practice.

(3) Dr Kim raises a very important point about the proportions of dry periods, about which we have not said anything in the paper.

The parameter estimation process does not seem to have considered rainfall intermittency (e.g. equations for proportion of dry/wet period). If you put the parameter values of Table 4 for the equation of proportion of dry period, the value is almost 0, which means it rains all the time

Ans: It is indeed correct that the proportions of dry periods (proportion dry) have not been included in the model calibration. That makes them prime candidates for model validation according to the standard practice of stochastic model validation: this involves distinguishing between properties used in the calibration and properties used in validation (rather than splitting the observed data set into a calibration and a validation period).

The proportion of wet periods plots the referee shows in his review indicate some substantial overestimation of the proportions of wet periods, i.e. an underestimation of the proportion dry, by the model over a range of time-scales. This is in fact an issue that we had noted in carrying out model simulations and that can be discussed in both theoretical and sampling aspects.

According to the theoretical form of the proportion dry given in Rodriguez-Iturbe et al (1988) (see equation (2.5)) and its approximation given in Wheater et al. (2006) (see equation (B48) at page 412), we note that the constraint for α is $\alpha > 1$. The constraint for α is however $\alpha > 0$ in the new RBL2-sM-NC model, and, as summarised in Table 4 in the manuscript, the α values we obtained are mostly smaller than or very close to 1. Therefore, the theoretical proportion dry can hardly be derived using the approximate equation given in Wheater et al. (2006).

This issue can however be better addressed through sampling. We had found that the underestimation of the proportion dry is due to the generation of many tiny amounts of rainfall which are not significant for any hydrological application. If we therefore look rather at the proportion of near-dry periods (with rainfall below a small threshold of 0.01 mm per 5-min) the problem disappears at hourly and sub-hourly scales. A comparison is given in Figure 1 of proportion dry statistics derived from 250 simulations of RBL2-sM-NC, RBL2-sM and RBL2-bM models, respectively. As can be seen, the new RBL2-sM-NC can better reproduce proportion dry statistics at 5-min and 1-h timescales than RBL2-sM and RBL2-bM models. However, the RBL2-bM model start to outperform the other two models at multi-hour timescales.

Considering that the paper is already rather long, and we do not use proportion dry for model calibration, we opt for not including this in the main paper. However, we add this in the supplement (Section S1) and mention about this on lines 127-8 in the main paper. In the supplement, the theoretical proportion dry and its approximate equations are first given, and then the associated constraint for α is explained. In addition, the sampling result as shown in Figure 1 is included in S1.

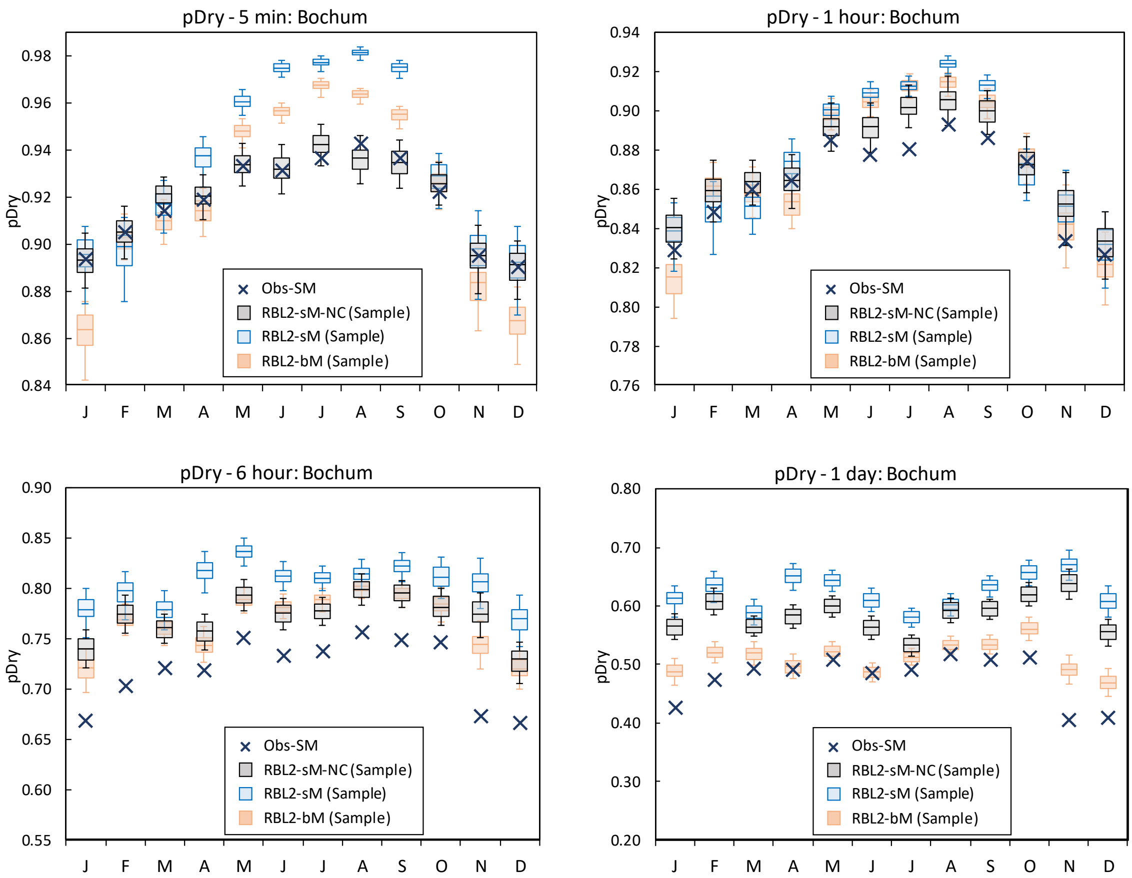

Figure 1: Proportion dry by month at Bochum: the observed vs. the fitted using RBL2 models with the original and the new solution spaces of α (RBL2-bM, light orange boxplots; RBL2-sM, light blue boxplots; RBL2-sM-NC, black boxplots).

(4) Dr Kim suggests specifying parameter units and objective function values in the tables.

Please specify the unit of the parameters in the tables. Especially, the parameter iota in the paper confused me because the original Bochum data is in the unit of cm and your iota is in the unit of mm. It may be also beneficial if you add the column of the objective function values in the tables for the reader's reference.

Ans: We thank Dr Kim for this suggestion. The units of the parameters have been added to the tables. In addition, a new table (similar to the one below) has been added, summarising the minimum objective function values (i.e. Table 5).

Note that the minimum objective function values of the RBL2-bM model in Kaczmarska et al. (2014) (see Table 2) are given here (in grey font colour). This is to demonstrate that the minimum objective function values obtained in our work are similar to those obtained in the previous research. It is also worth noting that the minimum objective function values of the RBL2-sM-NC model are much lower than those of the RBL2-sM model.

Model	Jan	Feb	Mar	Apr	May	Jun	Jul	Aug	Sep	Oct	Nov	Dec
RBL1-bM	85.6	66.8	89.4	93.3	127.9	105.8	107.6	126.6	114.2	92.1	102.9	83.8
RBL2-bM	39.5	30.1	52.1	56.2	73.0	65.2	65.6	72.8	60.4	47.0	41.0	36.6
RBL2-bM*	39	22	46	63	74	76	92	74	68	47	23	26
RBL1-sM	227.5	176.7	192.1	169.1	221.9	328.5	180.3	620.3	323.9	110.1	280.4	410.0
RBL2-sM	145.0	76.7	117.6	173.6	174.3	315.6	96.5	478.4	241.6	61.2	244.6	280.5
RBL1-sM-NC	186.5	169.9	192.0	149.4	221.9	328.5	180.3	620.3	323.9	107.5	104.0	348.8
RBL2-sM-NC	37.4	23.7	75.7	60.9	43.7	59.1	8.2	32.9	8.5	32.4	109.2	142.6

* The minimum objective function values are obtained from Table 2 in Kaczmarska et al. (2014)

(5) Dr Kim indicates that using another numerical method, better parameters can be obtained.

I could estimate the better parameter values with the particle swarm optimization algorithm (less underestimation of variance and skewness, and the P0 aligning to 1:1 line)

Ans: Again, we thank Dr Kim for his work in reviewing this paper, which amounts to a very thorough and useful investigation. There are two issues here. First, as Dr Kim points out, the objective functions obtained when calibrating these Poisson-cluster rectangular pulse models are highly non-linear and are likely to have many local optima. He is therefore right to point out that non-traditional numerical methods such as Particle Swarm optimisation are likely to be very useful to avoid an iterative algorithm converging to a non-global local optimum. Second, however, the statistics used in the fitting by Dr Kim are different from the ones we used – and in particular, they are likely to include the proportion dry. Aside from the issue of improved reproduction of the proportion dry, we would have to look at whether the other statistics are significantly improved.

Based upon Dr Kim's results, we agree that, in this case, Particle Swarm optimisation is a better solver than our numerical method that, as described in the paper, combines the Simulated Annealing and the downhill simplex Nelder-Mead algorithms, but we note that the objective functions we obtained are comparable to those obtained in Kaczmarska et al. (2014) – we add a comment about this on lines 143-4. We are keen to try the Particle Swarm optimisation method in our future work. However, we would like to highlight that the main contribution of this paper is the re-investigation of the key parameter constraint for the RBL models and the associated new formulation; and we believe that the impact of this change in preserving sub-hourly extreme statistics is likely to be more significant than that resulting from a better numerical solver.

(6) Dr Kim raises an interesting point about the fact that there seems to be a difference in the role that the proportion dry and the proportion wet would play in the objective function, when we use the weights that are recommended for these generalised methods of moments.

Let's say that we consider the proportion of dry period (P0) in the calibration process. The interannual variability of P0 will be very small because it is one minus small value every year (e.g. 0.998, 0.980, 0.950, etc.). Therefore, it will have very high weight. Let's say we consider the proportion of wet period (PW) in the calibration process. The interannual variability will be greater than the first case (e.g. 0.002, 0.020, 0.050, etc.)

Ans: I think there is a misconception here in thinking that the variability of the proportion dry will be different from that of the proportion wet. Indeed, we always have $Var(1-X) = Var(X)$ so if X is the proportion dry, then $1 - X$ is the proportion wet, and they both have the same variance, and will therefore be given the same weight in the objective function.

(7) Dr Kim makes a point about the block estimates

Regarding the block estimation, the mean of the block values are the estimates of the true statistics, which we can get easily, so I think the parameter estimation should always be performed based on the true statistics

Ans: We agree with the last part of the statement if 'true statistics' means 'best available estimates of the population statistics' in some sense of best (probably including non-biased, maybe also with minimal variance). But the block estimation method introduces some bias for instance.

References

Kaczmarska, J., Isham, V., and Onof, C.: Point process models for fine-resolution rainfall, Hydrological Sciences Journal, 59, 1972–1991, https://doi.org/10.1080/02626667.2014.925558, 2014.

Rodriguez-Iturbe, I., Cox, D. R., and Isham, V.: A point process model for rainfall: further developments, Proceedings of the Royal720Society of London A: Mathematical, Physical and Engineering Sciences, 417, 283–298, https://doi.org/10.1098/rspa.1988.0061, http://rspa.royalsocietypublishing.org/content/417/1853/283, 1988

Wheater, H. S., Isham, V. S., Chandler, R. E., Onof, C., Bellone, E., Prudhomme, C., and Crooks, S.: Improved methods for national spatial-temporal rainfall and evaporation modelling for BSM, Tech. Rep., DEFRA, randd.defra.gov.uk/Document.aspx?Document=FD2105_6227_PR.pdf, 2006.

Reply to Referee #2

We thank Referee #2 for her/his positive comments. We agree that this is indeed quite a remarkable dataset to have access to. We also agree that this work is relevant to a wide range of applications beyond flood design.

(1) The referee makes an important comment about the context setting in the paper.

The paper would benefit greatly from additional material setting out the scope and extent of previous applications for this family of models. The paper is written for the cognoscenti, but for those not deeply familiar with the models, more context would provide helpful motivation, i.e. lines 14 -19 should be expanded.

Ans: We thank the referee for pointing that out. The paper is indeed light on information about the applicability of these models. We therefore add some sentences to provide further context setting to motivate the work and show its importance in relation to applications (lines 15-24).

(2) The two other minor comments made by the referee are addressed by making the required changes in the text.

- Line 64: This sentence has been changed to: *The other issue, namely that of the reproduction of the variability of rainfall depths across scales, had not so far received much attention although it is in fact of clear practical import.*
- Line 129: This sentence has been changed to: *The models are* ***generally*** *calibrated....*

Reply to Referee #3

We thank Referee #3 for her/his detailed comments on the paper.

Two important sets of issues are raised, and in both cases, we thank the referee for a careful reading of the paper which brings up issues that certainly need to be addressed if the message in the paper is to be conveyed clearly.

A. Derivations of the equations for moments of the rainfall depth.

A.1. The reviewer argues that no separation of integrals occurred in the original papers and that the condition on α remains valid (i.e. that it must be larger than 1):

In the model structure however, each storm has a different value of η. In Rodriguez-Iturbe et al. (1988), the derivation of the variance and covariances does not make use of separate integrals as claimed in the present paper: it just uses the expectation of $exp(-\eta\varphi\tau)/\eta$ where τ is a temporal lag; and (correctly) notes that this expectation exists only when $\alpha > 1$. It therefore looks to me as though the apparent problem noted by the present authors may be an artefact of an incorrect — or, perhaps, needlessly complicated — approach to the derivation.

Ans: There is a misunderstanding as to what is meant by the separation into a sum of integrals. We agree with the reviewer as to how the moments are calculated. As explained in the paper, the moment from the non-randomised model is multiplied by the density function of the Gamma distribution for η which gives rise to integrals of quantities involving terms such as $exp(-\eta\varphi\tau)/\eta$ over η (in fact this is just as described in Kaczmarska et al. (2014) which the lead author was a co-author of). This is possible because the terms in η involve only one storm (if one integrates the centred moments). We agree with all this.

However, when looking at these integrals involving terms such as $exp(-\eta\varphi\tau)/\eta$, there are in fact several such terms that are added. For instance, if one looks at the first time these equations were derived, in the paper the referee refers to (Rodriguez-Iturbe et al., 1988), the derivation clearly involves separating a couple of integrals. This can be seen by looking at equation (2.2): the expectation that is calculated is obtained by separating into additive terms and taking the expectation of each of these terms (thus integrating each additive term separately). So far, as the reviewer implies, each such term has been integrated separately. But in defining the domain of validity of the integration, what has thereby been assumed is that, when the individual integrals diverge, so does the integral of the sum of the terms (so that they have the same domain of validity over α). In this paper, we show that this is not the case.

That is, the important point to note is the simple one that the integral of a sum of terms is only equal to the sum of the integrals of each additive term when the latter are finite. When the latter are infinite (which, for the equation in question happens for $\alpha \leq 3$, because the pdf of the Gamma distribution is multiplied by this term), this is not necessarily the case. That is, it is, in general, possible that the integral of the sum should be finite while the integrals of the additive terms are infinite.

Here is an example to illustrate this issue. Consider the integral:

$$I = \int_0^x \frac{e^{\omega t} - e^{-\sigma t}}{t}\, dt$$

If we consider the sum of the two integrals:

$$I_1 = \int_0^x \frac{e^{\omega t}}{t}\, dt \text{ and } I_2 = \int_0^x \frac{-e^{-\sigma t}}{t}\, dt$$

we have two divergent integrals and we cannot say what this sum is $(+\infty - \infty)$.

But $I \neq I_1 + I_2$ because, using Taylor expansions, we see that I is in fact finite:

$$I = \int_0^x \frac{1 + \omega t - 1 + \sigma t + o(t)}{t}\, dt = \int_0^x \big(\omega + \sigma + o(1)\big)\, dt$$

So, for x small:

$$I \cong (\omega + \sigma)x$$

This situation is analogous to that in the paper, with $x = \eta_0$. That is, we have shown that the integrand can be approximated by sums of Taylor series which, in the neighbourhood of $\eta = 0$ have terms that cancel out, so that the convergence of the integral as a whole is not defined by the convergence of the expectation of $exp(-\eta\varphi\tau)\,/\eta$ or $exp(-\eta\tau)\,/\eta$. As we show in the paper, in the vicinity of $\eta = 0$, the integrand of the variance of the RBL1 model is a term in $\eta^{\alpha-2}$ which converges as long as $\alpha > 1$.

To avoid this misunderstanding, we add some text (lines 207-210) in the main part of the paper and a section in the Appendix (lines 666-686) to explain the key point that one cannot just treat integrals of additive terms separately when they are infinite.

A.2. The referee then raises a good point about the results found by previous authors and the claim that we make that they could be erroneous.

the authors' reporting of previous results with "non-valid" estimates for the α parameter (lines 178–181) should have made them stop and think more carefully. The reason is that the model fits are obtained by minimising an expression involving the theoretical model properties. Earlier authors must have calculated the properties for these values of α, therefore; but this wouldn't be possible if the integrals diverged (or the algebraic expressions would have produced results that are obviously wrong, such as negative values of $E(X^2)$).

Ans: There are two senses in which previous results might have been erroneous. The first, and most important one is that the domain of valid values of α was smaller than it need be in cases where the authors used the restrictions upon α required by the separate integration of the additive terms. This is the main reason for the work in this paper: it will allow a broader domain of values of α to be used.

But second, and this is the case that the referee is alluding to, the issue of convergence of the integrals was often not addressed by the authors (including some published with one of the present authors as co-author). This would however not necessarily be picked up when carrying out the optimisation, because all it means is that the expression for the corresponding moment would not have had a numerical value that was that of the model skewness. This would not have involved any negative numbers (only in some exponents). So, for instance, if we look at the claim we made on lines 173-179, we are drawing attention to the fact that, for the convergence of variance and covariance of the RBL1, the condition $\alpha > 3$ is required. The papers listed have some parameters smaller than 3. How does that translate in terms of the kind of quantities these authors would have found for, say, the variance. Well, if we look at the equation for the variance they would have used (see lines 203-205), it involves some values of the function T: $T(2, \ldots, \ldots)$ and $T(3, \ldots, \ldots)$. Going back to the definition of this function T (lines 157-158), we see that when α is less than 3, the term in the denominator, i.e. $(\nu + u)^{\alpha-k}$ has an exponent $\alpha - k$ which is $\alpha - 2$ for $k = 2$ and $\alpha - 3$ for $k = 3$. These exponents are less than 1 when $\alpha \leq 3$. But we will, as the referee points out, get some negative terms because of the negative $\alpha - 3$ but overall, we find positive variances. For instance, looking at the parameters A_1 and A_2 found by Rodriguez-Iturbe et al. (1988),

$$A_1 = \frac{\lambda \mu_C \nu^\alpha}{(\alpha-1)(\alpha-2)(\alpha-3)} \left[E(X^2) + \frac{\kappa \varphi \mu_X^2}{\varphi^2 - 1} \right]$$

$$A_2 = \frac{\lambda \mu_C \kappa \mu_X^2 \nu^\alpha}{\varphi^2(\varphi^2-1)(\alpha-1)(\alpha-2)(\alpha-3)}$$

we find that term A_1 on p.288 of that paper is negative when $1 < 2 < \alpha < 3$, while A_2 is positive. This will in fact generally be the case as can be seen from the following reasoning. Recall that φ is the ratio of the mean cell duration in the storm and the mean duration of storm activity. In practice (by which I mean, for a physically realistic set of parameters), we will therefore have $\varphi < 1$. From this we can conclude that $A_2 > 0$ when $1 < 2 < \alpha < 3$.

Next, consider κ: we will in practice have $\kappa > \varphi$, because κ is the ratio of the mean cell duration in the storm and the mean cell interarrival time in the storm, whereby the latter is less than the mean duration of storm activity. With these relations, we can show that the terms in square brackets is positive, and therefore $A_1 < 0$. Starting with the fact that $E(X^2) > \mu_X^2$ since the difference between left- and right-hand side is the variance of the cell depth X, we can then write the following for the terms in square brackets:

$$E(X^2) + \frac{\kappa \varphi \mu_X^2}{\varphi^2 - 1} = E(X^2) - \frac{\kappa\varphi}{1-\varphi^2} \mu_X^2 > E(X^2)\left(1 - \frac{\kappa\varphi}{1-\varphi^2}\right)$$

since the coefficient of μ_X^2 is negative. Further, we get:

$$E(X^2)\left(1 - \frac{\kappa\varphi}{1-\varphi^2}\right) = E(X^2)\left(\frac{1-\varphi^2-\kappa\varphi}{1-\varphi^2}\right) > E(X^2)\left(\frac{1-\varphi^2-\kappa^2}{1-\varphi^2}\right) > E(X^2) > 0$$

The expression for the variance is:

$$\begin{aligned}\operatorname{var}\left(Y_i^{(h)}\right) = {} & 2A_1\{(\alpha-3)h\nu^{2-\alpha} - \nu^{3-\alpha} + (\nu+h)^{3-\alpha}\} \\ & - 2A_2\{\varphi(\alpha-3)h\nu^{2-\alpha} - \nu^{3-\alpha} + (\nu+\varphi h)^{3-\alpha}\}\end{aligned}$$

in which we have just shown that $A_1 < 0$ and $A_2 > 0$.

The terms in curly brackets are both negative for the parameters we have looked at. The key to the sign of the variance will therefore be the relative sizes of $|A_1|$, $|A_2|$ and of the associated curly bracket terms (denote $|C_1|$ and $|C_2|$ here). Values for these expressions with a typical parameter set for which $2 < \alpha < 3$ are given in Table 1. As can be seen, with typical parameter values: $|A_1| < |A_2|$ and $|C_1| \gg |C_2|$. Therefore, we still get a positive expression for the variance. This means that this would not be picked up as anomalous in calibrating the model.

To clarify these issues, we differentiate the two related problems (line 202) and emphasise the one about non-optimality because of an unnecessarily narrow parameter space (which is currently not sufficiently clear in the paper). Since we cannot estimate the impact of the second problem without looking at the particular data sets used in past papers, we rephrase the comment we make about previous studies so that it indicates that one cannot be sure that the parameters found in these previous studies are optimal (lines 206-210). We also add a sentence about the fact that the issue would not have been noticed as it would probably not have led to negative variances for instance (lines 199-202).

Table 1: Calculations of the variance expression, given in Rodriguez-Iturbe et al. (1988), and the associated parameters at 1-h timescale ($h = 1$) for $2 < \alpha < 3$. Other parameters used are $\lambda = 0.025$, $\mu_x = 1.3$, $\nu = 0.28$, $\kappa = 0.65$ and $\varphi = 0.04$.

α	C_1	A_1	$C_1 \times A_1$	C_2	A_2	$C_2 \times A_2$	$\mathrm{var}\left(Y_i^{(h)}\right)$
2.1	-1.0871	-1.0031	1.0904	-0.0003	206.7770	-0.0574	2.2958
2.2	-1.1085	-0.4554	0.5048	-0.0006	93.8752	-0.0524	1.1145
2.3	-1.1159	-0.2820	0.3147	-0.0008	58.1307	-0.0482	0.7257
2.4	-1.1048	-0.2017	0.2229	-0.0011	41.5858	-0.0445	0.5348
2.5	-1.0703	-0.1592	0.1703	-0.0013	32.8071	-0.0414	0.4234
2.6	-1.0060	-0.1368	0.1377	-0.0014	28.2088	-0.0386	0.3526
2.7	-0.9046	-0.1296	0.1172	-0.0014	26.7155	-0.0362	0.3069
2.8	-0.7573	-0.1415	0.1071	-0.0012	29.1578	-0.0340	0.2823
2.9	-0.5533	-0.2098	0.1161	-0.0007	43.2381	-0.0321	0.2963

A.3. The referee proposes a simplification of the equations by using the fact that ratios of Gamma functions can lead to simpler expressions.

The authors' concerns about convergence are all focused on the situation where $l = 0$, because this is where the integrand can become infinite. In this case however, the final numerator in the expression above is a complete gamma function so that the expression can be written as

$$\Gamma(k,u,l) = \frac{\nu^\alpha}{(\nu+u)^\alpha}\frac{\Gamma(\alpha-k)}{\Gamma(\alpha)}$$

But if $k > 0$ is an integer (which I think it is throughout the paper), we have $\Gamma(\alpha)/\Gamma(\alpha-k) = (\alpha-1)(\alpha-2)\ldots(\alpha-k)$ providing $\alpha - k$ isn't a negative integer (if it is, then $\Gamma(\alpha-k)$ is undefined). Thus

$$\Gamma(k,u,l) = \frac{\nu^\alpha}{(\nu+u)^\alpha(\alpha-1)\ldots(\alpha-k)}$$

which is obviously finite providing none of the terms in the denominator is zero. Unless I've missed something, this seems to resolve the convergence issue much more simply.

Ans: This simplification is indeed well known and indeed, going back again to the Rodriguez-Iturbe et al., (1988), it was used for instance in equation (2.4): this is why no Gamma functions appear in the expressions of coefficients A_1 and A_2, but rather products such as $(\alpha - 1)(\alpha - 2)(\alpha - 3)$.

As the referee notes we can only use the Gamma function (and the simplifications that follow) when the variable in the Gamma function is non-negative (there is actually an extension of the Gamma function to negative non-integer numbers, but there is no obvious justification for using it: the Gamma function is introduced in the calculations because of the Gamma distribution, which requires positive parameters). This means, as stated by the referee that $\Gamma(\alpha - k)$ is defined as long as $\alpha > k$. This is precisely the issue that our paper is dealing with: this condition arises when calculating the integrals separately, and unnecessarily restricts the domain of feasibility for the minimisation of the objective function. By not treating the integrals separately which leads to using these (complete) Gamma functions, we show that the domain of possible values of α is broader.

Since it is likely that some readers will also wonder why we did not use complete Gamma functions and the simplifications which ensue, we add a sentence to explain this (lines 181-3).

B. The block estimators

The referee points to the fact that we have not used the standard unbiased estimators of the variance and that, if the problem that we are flagging is that some previous authors have not done this, then it is not worth being discussed extensively, if at all.

The authors' second main point relates to the calculation of "block" statistics used for model calibration with uncertainty. They claim that the block estimators of variances and other quantities are biased (e.g. lines 257-260). However, the expressions that they give for these estimators are incorrect because there is no adjustment for degrees of freedom in the denominator in either case: the denominator in the first expression should be $N_y N_{m,h} - 1$ and that in the second expression should be $N_y (N_{m,h} - 1)$. In fact, Section 5.1 of their Jesus and Chandler (2011) reference (cited on line 244) discusses the need for careful treatment of small-sample biases: that discussion would probably be relevant to quantities such as the skewness coefficient, discussed by the present authors at lines 291-294. Jesus & Chandler did not discuss the variance specifically: I assume that this is because the form of an unbiased variance estimator is well-known so they didn't think it needed mentioning. If the variance expressions given by the authors are indeed in standard use, this is worrying: a decent journal is probably not the best place to draw attention to such a basic error, however. The bottom line is that there isn't necessarily a problem with block estimators per se; but (as with any other sophisticated technique) if you're going to use them then you need to do it carefully.

Ans: We fully agree that, indeed, if the issue were the bias that is introduced by using $N_g N_{m,h}$ rather than $N_g N_{m,h} - 1$ and $N_g (N_{m,h} - 1)$, then this would not be worth discussing. As the referee points out, the differences between estimators using the first rather than the second coefficients are of relevance to small samples.

However, we are not concerned with small samples here. The smallest sample that might be involved would be of size 30 (in the case of the daily time-scale, for the block estimation method, and for all other time-scales used in the fitting, they are considerably larger). The estimators which do not use the '-1' adjustments are biased (and we indicate that, at least for one of them, after equation (10)). We would not agree that they are 'wrong': they just have a bias that can be corrected by using the '-1' adjustments pointed out by the referee, but they are asymptotically unbiased. And for samples that are, at worst, of size 30, the bias is not of much practical relevance (e.g. typically a few percent).

Still, one might ask why we did not use the unbiased estimators in any case, to avoid introducing even such small biases. That is a good point which we should have indicated in the paper. The reason is that it leads to simpler expressions for the comparison of the standard and block estimators. So, we get an equation (10) in which one can easily interpret the difference between the block estimator and standard estimator in terms of an additional term that is the variance of the monthly averages. In effect, this result is just the well-known result expressed in terms of sums of squares in ANOVA (e.g. see Kottegoda and Rosso (2008), p. 285). Since the reason for putting in this equation is just to give some understanding of where the differences between the estimators comes from, this seems sufficient for that purpose. Ultimately, significant differences between block and standard estimators only arise when dealing with ratios, as we explain in the paper, and for these, there are no useful such equations to write down.

In fact, the numerical estimates that we have shown are for the unbiased estimators, so that removes any concern about the impact of the biases in question. However, this points to the fact that we need to clarify these issues in the paper which, as currently presented, can be confusing. We therefore add some text to indicate that for the biased (but asymptotically unbiased) estimators of the variances, we get the relations shown in the equations, while the relations are a little more complex when using unbiased estimators. We also add a sentence to indicate that the numerical values are for unbiased estimators (lines 274-8). We also indicate that this brief investigation is not aimed at making any general point about block estimators, but simply indicating the problems that arise in the case of the estimator of a ratio like the coefficient of skewness (lines 271-2).

References

Kottegoda, N.T. and Rosso, R. (2008) *Applied Statistics for Civil and Environmental Engineers*, 2nd ed., London: Blackwell

Rodriguez-Iturbe, I., Cox, D.R., Isham, V. (1988) A point process model for rainfall: further developments*, Proc. Roy. Soc. Lond.*, A417, 283-298

Modelling rainfall with a Bartlett-Lewis process: New developments

Christian Onof[1] and Li-Pen Wang[1]

[1]Department of Civil and Environmental Engineering, Imperial College London, SW7 2AZ, UK

Correspondence: Christian Onof (c.onof@imperial.ac.uk)

Abstract. The use of Poisson-cluster processes to model rainfall time series at a range of scales now has a history of more than 30 years. Among them, the Randomised (also called modified) Bartlett-Lewis model (RBL1) is particularly popular, while a refinement of this model was proposed recently (RBL2) (Kaczmarska et al., 2014). Fitting such models essentially relies upon minimising the difference between theoretical statistics of the rainfall signal and their observed estimates. The first are obtained using closed form analytical expressions for statistics of order 1 to 3 of the rainfall depths, as well as useful approximations of the wet-dry structure properties. The second are standard estimates of these statistics for each month of the data. This paper discusses two issues that are important for optimal model fitting of the RBL1 and RBL2. The first is that, when revisiting the derivation of the analytical expressions for the rainfall depth moments, it appears that the space of possible parameters is wider than has been assumed in the past papers. The second is that care must be exerted in the way monthly statistics are estimated from the data. The impact of these two issues upon both models, in particular upon the estimation of extreme rainfall depths at hourly and sub-hourly timescales is examined using 69 years of 5-min and 105 years of 10-min rainfall data from Bochum (Germany) and Uccle (Belgium), respectively.

1 Background

Rainfall is the main input to a range of models in geophysics such as hydrological catchment models, sewerage discharge models, erosion models. Therefore, to understand the behaviour of catchment runoff, sewer flows or soil erosion, it is necessary to have access to precipitation data sets at the characteristic response scales of these variables. There are also other non-geophysical applications which require such data sets, for instance the investigation of the frequency of outages in telecommunications data. For all such applications, hourly and sub-hourly rainfall data are required. The availability of data sets that are long enough to represent the range of variability of precipitation at such scales is however limited, even in developed countries. This is why the availability of a stochastic model able to generate realistic time-series of rainfall depths at a range of scales is very useful. There is already a considerable literature in this area (Connolly et al., 1998; Arnbjerg-Nielsen, 2012; Arnbjerg-Nielsen et al., 2013; Onof and Arnbjerg-Nielsen, 2009; Wang et al., 2010): the present paper is a contribution to the improvement of the performance of a particular type of stochastic rainfall model.

Depending upon the application, 'realistic' will mean different things. For applications that are related to design, 'realistic' will involve the reproduction of the observed extreme behaviour of the precipitation process at a range of time-scales. Onof and Arnbjerg-Nielsen (2009) and Arnbjerg-Nielsen (2012), for example, integrated two stochastic models to eventually generate 5-min point rainfall time series from 1-h 10-km RCM (Regional Climate Model) output. This method enables the consideration of the impact of climate change in urban sewer system design.

In this paper, we focus upon one approach to rainfall modelling, that which is based upon the use of point processes as defining the times at which the building blocks of the model, i.e. rainfall cells, arrive. These cells are conceptual ones, although their typical characteristics are those of Small Mesoscale Areas (SMSA) which are embedded in Large Mesoscale Areas (Burlando and Rosso, 1993). The presence of clustering means that a homogeneous Poisson point process is not an appropriate choice for the underlying process of cell arrivals. Two options are available. The first introduces randomness by having the Poisson rates behave as a continuous-time Markov chain: this defines a Cox (doubly-stochastic) process (see Ramesh (1995); Ramesh et al. (2018)).

The second explicitly models the clustering process. This can be by defining the number cells in a storm as a random variable, with another random variable modelling the delays from the storm to the cell arrival time. This defines a Neyman-Scott process (see Cowpertwait (1998); Evin and Favre (2008); Paschalis et al. (2014)). Alternatively, a second homogeneous Poisson process defines the cell arrival times over a duration of storm activity that defines a random variable (see Onof and Wheater (1993); Khaliq and Cunnane (1996); Verhoest et al. (1997); Kossieris et al. (2018)). For both Poisson-cluster processes, the SMSAs are then represented by rectangular pulses corresponding to a random constant rainfall intensity over a random duration. In this paper, the Bartlett-Lewis process is the chosen point process model.

Two issues have been flagged in the literature which limit the applicability of a number of variants of the basic model type published in 1987 (Rodriguez-Iturbe et al., 1987). The first one is well-known (e.g. Verhoest et al. (2010)). Many studies have shown that Rectangular Pulse models underestimate hourly extremes (Verhoest et al. (2010) and references therein). This is often accompanied by an overestimation of daily extremes. The other, less well-known problem was identified by Marani (2003). While one of the strengths of models based upon Poisson-cluster processes is their ability to capture rainfall variability over a range of scales (hence its use in disaggregation - see Koutsoyiannis and Mamassis (2001)), they underestimate this variability for scales equal to or larger than a few days.

Both issues are closely connected to fundamental features of these models and of the way they are fitted. The first arises partly due to the fact that the model is calibrated in such a way as to reproduce the mean behaviour of the precipitation process. That is, statistics like the mean, variance, autocovariance of rainfall totals at time-scales varying from one to 24 hours are used to fit the models. As far as the cell intensity parameters are concerned, these statistics are functions of their first and second-order moments only. The rest of this distribution is not thereby determined, although the choice of distribution has a clear impact upon the extremes (Onof and Wheater, 1994). This situation can be partially addressed by including the coefficients of skewness (hereafter, 'skewness') of the rainfall depths at relevant time-scales as additional statistics in the calibration of the model (Cowpertwait, 1998). Kaczmarska et al. (2014) similarly find that the inclusion of the skewness yields a reasonable performance and extend the range of time-scales to include sub-hourly scales which are of key importance in urban hydrology, erosion studies and telecommunications applications. There remains however the option of using a fat-tailed distribution for the cell intensity to achieve further improvement. To see whether this is advisable/useful, we need to get a better picture of what produces the extremes at different time-scales: is it predominantly the superposition of several cells, or is it mostly the rainfall produced by a single cell. In the latter case, the choice of a different distribution of rainfall intensities is a key decision.

The other issue, namely that of the reproduction of the variability of rainfall depths across scales, had not so far received much attention although it is in fact of clear practical import. If we want the model to be able to capture longer term variability (as would certainly be required to reproduce climate variability for instance), then this issue must be addressed. The most promising ways forward in this respect come from combining the Poisson-cluster model with a coarse-scale model that captures much of the longer-term variability (Park et al., 2019), or from letting climatological information guide the weighting to be assigned to different months in the data in calibrating the model (Kaczmarska et al. (2015); Cross et al. (2019)). Both approaches represent important developments. The first approach involving the combination of two models has the advantage of enabling a much improved reproduction of extreme rainfall depths. The second approach which incorporates climatological information, enables this model to be used as weather generator in climate impact studies.

While the use of extraneous (e.g. climatological) information and the combination with another (e.g. coarse-scale) model are the most promising ways in which this area of stochastic rainfall modelling is developing, the issue of how the Poisson-cluster model is fitted to rainfall statistics needs to be revisited. In this paper, we address two hitherto unnoticed issues with random parameter Bartlett-Lewis rainfall models. First, we draw attention to a claim made in the original publication of the randomised Bartlett-Lewis model (Rodriguez-Iturbe et al., 1988) which involves an erroneous assessment of the mathematically feasible limits of a key model parameter. Correcting this misspecification of the constraints on this parameter allows us to consider a broader parameter space, thereby potentially including parameter values that will improve model performance. Second, we show the importance of the choice of estimators for the statistics used in model fits to individual months. We shall show that, by taking both issues into account, it is possible to improve the reproduction of extreme rainfall depths over a range of scales. A detailed examination of the impact upon the variance function will be carried out in another paper.

This paper starts with a presentation of the data and a reminder of the structure of three versions of the Rectangular Pulse Bartlett-Lewis model, as well as of how these models are fitted. The revised equations for the statistics of order 1 to 3 of the rainfall depths at aggregation scale h hours are then presented. In the following section, we discuss the estimation of standard monthly statistics, and show the bias that can be introduced through the use of a commonly used type of estimator. In the final section, we consider the impact of the new equations and unbiased estimation method upon the reproduction of standard statistics and extremes of rainfall depths.

2 Data

Five-minute rain gauge rainfall data from a rain gauge in Germany (North-Rhine-Westphalia) and one in Belgium (Flanders: Brussels region) are used to demonstrate the new developments in model (population) and data (sample) statistics for model fitting described in this paper. These are:

- Bochum: 69 years of 5 minute data from January 1981 to December 1999;
- Uccle: 105 years of 10 minute data from January 1898 to December 2002.

Because of constraints on the length of the paper, the results for Uccle are shown only in the Supplement of this paper.

Additionally, for the purpose of the numerical investigation of estimators, Greenwich (14.5 years of 5 minute data from February 1987 to July 2001) data are used.

3 Model structure

In the original Bartlett-Lewis Rectangular Pulse (OBL) model (as illustrated in Fig. 1), storms arrive according to a Poisson process at rate λ. Another process generates cells associated with each storm: this is also a Poisson process, triggered by the storm arrival (rate β), and active over a duration that is exponentially distributed with parameter γ. These cells have an exponential duration (parameter η) and a random depth (described by its first three (non-centred) moments: μ_x ; μ_{x2}; μ_{x3}).

Further development of the original model proposed by Rodriguez-Iturbe et al. (1987) involved has in particular focused upon the randomisation of the temporal structure of storms for the Bartlett-Lewis process (Rodriguez-Iturbe et al., 1988; Onof and Wheater, 1993). The temporal structure of precipitation is allowed to vary from storm to storm by randomising parameter η. This can be chosen as a $\Gamma(\alpha, 1/\nu)$ distributed random variable that varies between storms. The cell arrival rate and storm duration parameter are scaled accordingly: $\beta = \kappa\eta$; $\gamma = \phi\eta$. This will be referred to as the Randomised Bartlett-Lewis model version 1 (RBL1).

Recently, this randomisation strategy was extended to include all the parameters describing the internal structure of the storm, i.e. to include parameter μ_x (Kaczmarska et al., 2014). μ_x is now a random variable that takes on different values for different storms, proportionally to η: $\mu_x = \iota\eta$. This is the Randomised Bartlett-Lewis model version 2 (RBL2). This model was shown to outperform the OBL and RBL1 by Kaczmarska et al. (2014), but:

- only one data set was examined in that study so this conclusion cannot be generalised;
- the RBL1 was excluded from the comparison because the authors 'concluded that the improvement in the fit to proportion dry that had previously been found by randomizing η was at the expense of a deterioration in the fit to the skewness' (ibid.); but given the popularity and successful application of this model to a range of types of rainfall (e.g. see Onof et al. (2000)), we decided to include it here for further analysis.

4 Model calibration and the revised equations

4.1 Calibration

The OBL, RBL1 and RBL2 models generate rainfall as a continuous-time process, $\{Y(t)\}_{t\in\mathbb{R}}$: $Y(t)$ is the continuous-time rainfall intensity at time t resulting from the superposition of the intensities of all the cells active at time t. Rainfall records are, however, available in aggregated form for discrete time-scales.The rainfall depth $Y_i^{(h)}$ for a level of aggregation h hours is given by:

$$Y_i^{(h)} = \int\limits_{(i-1)h}^{ih} Y(t)\,dt \tag{1}$$

Analytical expressions of the moments of the aggregated process $Y_i^{(h)}$ have been derived as functions of the model parameters. Expressions for other statistical descriptors such as the proportion of dry periods at time scale h, have also been derived (see Onof et al. (2000)). In the Supplement to this paper, we provide more efficient approximations of the proportion dry than in the earlier papers (see Wheater et al. (2006)).

The models are generally calibrated using a Generalised Method of Moments. That is, the model parameters are chosen so that the model values calculated with the available analytical expressions are as close as possible to the empirical values of these statistics obtained from observed data. This is achieved by minimising an objective function:

$$\sum_{\mathcal{M}\in\Omega} \omega(\mathcal{M}) \left\{ \mathcal{M} - \hat{\mathcal{M}} \right\}^2 \tag{2}$$

where Ω is a set of statistical descriptors, $\omega(\mathcal{M})$ a weight assigned to that property in the objective function, and $\hat{\mathcal{M}}$ is the estimate of that property from the sample of available data. For details about the optimal choices of the weights, see Kaczmarska et al. (2014).

In this paper, following the best practise suggested in Kaczmarska et al. (2014), we choose mean 1-h rainfall depth, and coefficient of variation, autocorrelation lag-1 and coefficient of skewness at 5/10-min (5 min for Bochum, 10 min for Uccle), 1-, 6- and 24-hour time-scales as statistical descriptors for the model calibration. In addition, inspired by the optimisation method proposed in Efstratiadis et al. (2002), we used the Simulated Annealing algorithm to search a promising region, and then the downhill simplex Nelder-Mead algorithm to identify the optimum to minimise Eq. (2). The minimum objective function values for all the RBL models under consideration in this paper using Bochum data are summarised in Table 5. It is worth noting that the minimum objective function values of the RBL2-bM model are comparable with those of the BLRPRx model given in Table 2 in Kaczmarska et al. (2014), which indicates that there is consistency between the calibration procedures in these two papers.

Below, we present the methodology used to derive the new equations for the two randomised versions of the Bartlett-Lewis model.

4.2 Derivation of the new equations

As explained in Rodriguez-Iturbe et al. (1988), the mean and variance of the RBL1 - and this also applies to the RBL2 - are obtained by taking means over η of these moments for the OBL. This is the case because the expressions of these moments only contain terms corresponding to contributions from single storms, i.e. $\lambda^q \eta^p$ terms with $q = 1$ only, as can be seen from the equations obtained by Rodriguez-Iturbe et al. (1987). The same goes for the derivation of the third-order centred moment.

In this section, we focus upon the derivation of the variance of the RBL1. The complete sets of new equations for RBL1 and RBL2 are presented in Appendix A.

The starting point for the derivation is the equation for the variance of the OBL model. Here, rather than use the original OBL model parameters (Rodriguez-Iturbe et al., 1987), i.e.

$$\{\lambda, \gamma, \beta, \eta, \mu_x, \mu_{x^2}, \mu_{x^3}\}$$

We replace the second and third parameters by dimensionless parameters ϕ and κ that are also used in RBL1 and RBL2 so that the parameterisation of the OBL is now in terms of:

$$\{\lambda, \phi, \kappa, \eta, \mu_x, \mu_{x^2}, \mu_{x^3}\}$$

where $\gamma = \phi\eta$ and $\beta = \kappa\eta$.

In the analytical expression for the OBL variance, we make the dependence upon parameter η explicit by referring to it as $V(h,\eta)$, This distinguishes it from the corresponding variances for RBL models denoted $V(h)$. The OBL variance is:

$$\begin{aligned}
V(h,\eta) &= \frac{2\lambda\mu_c}{\eta}\left[\frac{(\mu_{x^2}+\kappa\mu_x^2/\phi)h}{\eta} + \frac{\mu_x^2\kappa(1-e^{-\phi\eta h})}{\phi^2\eta^2(\phi^2-1)} - \left(\mu_{x^2}+\frac{\kappa\phi\mu_x^2}{\phi^2-1}\right)\frac{1-e^{-\eta h}}{\eta^2}\right] \\
&= 2\lambda\mu_c\mu_x^2\left\{\left(f_1+\frac{\kappa}{\phi}\right)\frac{h}{\eta^2} + \left(\frac{\kappa}{\phi^2(\phi^2-1)}\right)\frac{1-e^{-\phi\eta h}}{\eta^3}\right. \\
&\quad \left. + \left(f_1+\frac{\kappa\phi}{\phi^2-1}\right)\frac{1-e^{-\eta h}}{\eta^3}\right\} \qquad (3)
\end{aligned}$$

where $f_1 = \mu_{X^2}/\mu_X^2$ and $f_2 = \mu_{X^3}/\mu_X^3$. For more on the choice of these parameters, see Appendix B.

When deriving the expression for a moment $\mathcal{M}$ in the RBL models, we multiply the corresponding moment $\mathcal{M}(\eta)$ for the OBL model by the density function f of the gamma distribution $\Gamma(\alpha, 1/\nu)$ of η and integrate over all possible values of η:

$$\mathcal{M} = E_\eta\left[\mathcal{M}(\eta)\right] = \int_0^\infty \mathcal{M}(\eta) f(\eta)\, d\eta \qquad (4)$$

where the density function of the Gamma distribution is given by:

$$\begin{aligned}
f(\eta) &= \frac{\eta^{\alpha-1}\nu^\alpha e^{-\nu\eta}}{\Gamma(\alpha)}\, d\eta \text{ if } \eta \geq 0 \\
f(\eta) &= 0 \text{ if } \eta < 0
\end{aligned}$$

The issue of the convergence of these integrals has, however, not been addressed explicitly in the literature (aside from a mention in Kaczmarska et al. (2014)). The integration involves integrals of the following general type evaluated at $l = 0$:

$$\begin{aligned}
T(k,u,l) &= \int_l^{+\infty} \eta^{-k} e^{-u\eta} \frac{\eta^{\alpha-1}\nu^\alpha e^{-\nu\eta}}{\Gamma(\alpha)}\, d\eta \\
&= \frac{\nu^\alpha}{(\nu+u)^{\alpha-k}} \frac{\Gamma(\alpha-k, l(\nu+u))}{\Gamma(\alpha)}
\end{aligned} \qquad (5)$$

where $\Gamma(s)$ is the (complete) Gamma function, and $\Gamma(s,x)$ the incomplete Gamma function, defined as:

$$\Gamma(s,x) = \int_{x}^{\infty} t^{s-1} e^{-t} \, dt$$

When $l = 0$, the integration in (5) is possible (i.e. the integral is finite) if and only if the integrand is integrable in the neighbourhood of 0, since there are no problems of convergence at ∞. And if the integration is possible for $l = 0$, the expression in (5) can be simplified using the properties of the Gamma function. This will however not be of use here, since we are not considering such integrals separately, as we shall see below.

If we look at the terms the integrand comprises for the statistics that are used to fit the model, we find that they behave in the neighbourhood of 0 as $\eta^{\alpha-n}$ with $n = 2$ for the mean rainfall intensity, $n \leq 4$ for its variance and covariance, and $n \leq 5$ for its third-order central moment. The integrals of such terms converge as long as $\alpha - n > -1$, i.e. $\alpha > n - 1$..

It therefore seems that, for the RBL1, $V(h)$ is finite as long as $\alpha > 3$. Similarly, as the expressions in A2 show, the mean $M(h)$ is finite as long as $\alpha > 1$, the covariance of lag k $C(k,h)$ is finite when $\alpha > 3$ and the third-order centred moment $S(h)$, when $\alpha > 4$.

This conclusion is however too hasty. Indeed, it involves considering separately the integration of each additive term in Eq. (3). It is with such separate integration that the expressions for the variance and covariance used in Rodriguez-Iturbe et al. (1988) are obtained, and these expressions were used in subsequent research.

Insofar as only moments of order less than 3 were used in past studies (the third-order moment for the RBL1 was only published in a report (Onof et al., 2013) and therefore not used in most of the literature), the constraint $\alpha > 3$ applied to the fits found in these past papers (e.g.(Rodriguez-Iturbe et al., 1988), (Khaliq and Cunnane, 1996), (Verhoest et al., 1997), (Onof et al., 2000), (Verhoest et al., 2010) and (Kim et al., 2017)). However, since the issue of the convergence of these integrals was not examined, it is not surprising to find, in most of these studies, that values of α below 3, i.e. outside the domain of feasibility of the optimisation, are obtained for some months. The parameter sets for these months are thus not feasible and *a fortiori* not optimal. Note that this issue would not easily have been picked up during model calibration because it would not typically have led to unrealistic values of these statistics. In particular, we found that, as long as we keep $\alpha < 2$ (as is the case in the literature), the variance remains positive for typical values of the other parameters.

But aside from this consequence, we now need to check whether, when proceeding without separating the integration into the sum of integrals of the additive terms in the integrand, the domain of convergence of the integral is still defined by $\alpha \in (3, +\infty)$ for the variance (and for the covariance, and $\alpha \in (4, +\infty)$ for the third-order moment). That is, are any values of α for which the individuals integrals diverge, but the integral of the whole integrand does not? That would be the case for instance if, in the neighbourhood of 0, the terms leading to a divergence for certain values of α were to cancel out (for a simple example of individual integrals diverging while, when summed, the total integral does not diverge, see Appendix C). Insofar as this is the case, as we shall see below, this will lead to a broadening of the space of feasible parameters as compared with what has been assumed in many studies, with new equations for the extended part of the parameter space. The consequence is that we cannot be certain that the parameters found in these previous studies are optimal.

In line with Eq. (4), the variance $V(h)$ of the RBL1 model is obtained as:

$$V(h) = \int_0^\infty V(h,\eta) f(\eta)\, d\eta \tag{6}$$

and if we choose a small value η_0 of η, this integral is the sum:

$$V(h) = \int_0^{\eta_0} V(h,\eta) f(\eta)\, d\eta + \int_{\eta_0}^\infty V(h,\eta) f(\eta)\, d\eta \tag{7}$$

whereby only the first integral has a limited domain of convergence. Let us call this first term $V_1(h)$.

From Eq. (3), we have:

$$\begin{aligned} V_1(h) \quad &= \quad \frac{2\lambda\mu_c\mu_x^2}{\Gamma(\alpha)} \int_0^{\eta_0} \left[\eta^{\alpha-3}\nu^\alpha e^{-\nu\eta} \left(f_1 + \frac{\kappa}{\phi} \right) h + \eta^{\alpha-4}\nu^\alpha e^{-\nu\eta} \left(\frac{\kappa(1-\phi^3)}{\phi^2(\phi^2-1)} - f_1 \right) \right. \\ &\quad \left. - \, \eta^{\alpha-4}\nu^\alpha e^{-(\nu+\phi h)\eta} \left(\frac{\kappa}{\phi^2(\phi^2-1)} \right) + \eta^{\alpha-4}\nu^\alpha e^{-(\nu+h)\eta} \left(f_1 + \frac{\kappa\phi}{\phi^2-1} \right) \right] \, d\eta \end{aligned}$$

By doing first and second-order expansions of the exponential terms, we find that the $\eta^{\alpha-4}$ and $\eta^{\alpha-3}$ terms cancel, so that after some algebra, we get:

$$V_1(h) \quad = \quad \frac{2\lambda\mu_c\mu_x^2}{\Gamma(\alpha)} \int_0^{\eta_0} \left[\eta^{\alpha-2}\nu^\alpha \frac{h^2}{2} \left(\frac{\kappa}{\phi+1} + f_1 \right) + o(\eta^{\alpha-2}) \right] \, d\eta$$

which yields:

$$V_1(h) \approx \frac{\lambda\mu_c\nu^\alpha h^2 \mu_x^2 \eta_0^{\alpha-1}}{(\alpha-1)\Gamma(\alpha)} \left(\frac{\kappa}{\phi+1} + f_1 \right) \tag{8}$$

as long as $\alpha - 2 > -1$, i.e. $\alpha > 1$. Else, $V_1(h)$ is infinite.

This second term $V_2(h)$ is thus calculated as:

$$\begin{aligned} V_2(h) \quad &= \quad \int_{\eta_0}^\infty V(h,\eta) f(\eta)\, d\eta \\ &= \quad 2\lambda\mu_c\mu_x^2 \left[\left(f_1 + \frac{\kappa}{\phi} \right) hT(2,0,\eta_0) + \left(\frac{\kappa(1-\phi^3)}{\phi^2(\phi^2-1)} - f_1 \right) T(3,0,\eta_0) \right. \\ &\quad \left. - \left(\frac{\kappa}{\phi^2(\phi^2-1)} \right) T(3,\phi h,\eta_0) + \left(f_1 + \frac{\kappa\phi}{\phi^2-1} \right) T(3,h,\eta_0) \right] \end{aligned}$$

so that the total variance is:

$$
\begin{aligned}
V(h) &= 2\lambda\mu_c\mu_x^2\left[\left(f_1+\frac{\kappa}{\phi}\right)hT(2,0,0)+\left(\frac{\kappa(1-\phi^3)}{\phi^2(\phi^2-1)}-f_1\right)T(3,0,0)\right.\\
&\quad\left.-\frac{\kappa}{\phi^2(\phi^2-1)}T(3,\phi h,0)+\left(f_1+\frac{\kappa\phi}{\phi^2-1}\right)T(3,h,0)\right]\\
&\quad\text{for } \alpha>3\\
V(h) &\approx 2\lambda\mu_c\mu_x^2\left[\frac{\nu^\alpha h^2\eta_0^{\alpha-1}}{2(\alpha-1)\Gamma(\alpha)}\left(\frac{\kappa}{\phi+1}+f_1\right)\right.\\
&\quad+\left(f_1+\frac{\kappa}{\phi}\right)hT(2,0,\eta_0)+\left(\frac{\kappa(1-\phi^3)}{\phi^2(\phi^2-1)}-f_1\right)T(3,0,\eta_0)\\
&\quad\left.-\left(\frac{\kappa}{\phi^2(\phi^2-1)}\right)T(3,\phi h,\eta_0)+\left(f_1+\frac{\kappa\phi}{\phi^2-1}\right)T(3,h,\eta_0)\right]\\
&\quad\text{for } 1<\alpha\leq 3\\
V(h) &= \infty\\
&\quad\text{for } \alpha\leq 1
\end{aligned}
\tag{9}
$$

In practice, η_0 should be chosen as small as is computationally possible since it is term $V_1(h)$ that involves the approximation. Figure 2 shows, for some typical parameter values, how sensitive the expressions of $V(h)$ (blue line), as well as $C(1,h)$ and $S(h)$ (grey and orange lines; and see derivations below), are to the choice of η_0. As can be seen, values start to be much less insensitive to the change of η_0 as $\eta_0 < 0.01$. In this paper, $\eta_0 = 0.001$ is chosen.

As indicated, similar derivations yield the expressions for the covariance of lag-k $C(k,h)$ and the centred third-order moment $S(h)$ of the RBL1.

For the RBL2, μ_x is now random, and chosen proportional to η: $\mu_x = \iota\eta$ so that shorter cells will tend to have greater intensity. The model equations for the RBL2 are therefore obtained from those of the OBL by, first, substituting $\iota\eta$ for μ_x in the expressions for the OBL model moments, and then proceeding as for the RBL1, i.e. integrating these moments multiplied by the density function of the gamma distribution of η. For this model, the constraint upon α obtained when carrying out separate integrations of the additive terms for the moments of the rainfall depth is less stringent than for the the RBL1. If we look at terms the integrands comprise, we find that, for the RBL2, they behave in the neighbourhood of 0 as $\eta^{\alpha-n}$ with $n=1$ for the mean, $n\leq 2$ for the variance, covariance and the third-order moment. The integrals of such terms converge as long as $\alpha-n>-1$, i.e. $\alpha>n-1$.

Analogously to the RBL1, it therefore seems that $M(h)$ is finite as long as $\alpha>0$, $V(h)$, $C(k,h)$ and $S(k,h)$ are finite as long as $\alpha>1$. But this conclusion is only warranted for the mean. For the other statistics, Taylor expansions of the exponential terms in the neighbourhood of 0 yield approximations for which the integrals are finite for certain values of α for which the individual additive terms are not integrable. The results are shown in Appendix A3.

5 Model calibration and the estimation of standard statistics

5.1 Standard or block estimation?

In fitting Poisson-cluster models, it is standard to consider parts of the year separately e.g. seasons or generally months, and to estimate parameter sets for each of these parts. These parts define blocks of data in the full time-series of observed rainfall. The question then arises as to how to deal with data presenting this block structure. The approach used in many papers, and certainly that which was implemented in the early papers that used data from the whole year (e.g. Onof and Wheater (1993)), consisted in treating the data between the blocks of interest (e.g. those corresponding to a given calendar month) as missing data. The standard estimators were then used for the moments of orders 1 to 3 and the proportions of wet periods at the time-scales of interest.

Work on the representation of the uncertainty in the model parameters (Wheater et al., 2006) and on the optimal weights to be used in the generalised method of moments implemented in the fitting (Jesus and Chandler, 2011) involved calculating statistics for each block of data of interest (e.g. each month of a given calendar month). This led to the use of other estimators, which we refer to as block estimators of the rainfall statistics. These are obtained by calculating the standard statistic of interest for each block and averaging over the blocks (e.g. each month of a given calendar month). The purpose of this section is to investigate the impact this might have upon the type of statistics used in Poisson cluster rectangular pulse model calibration, not to make any more general point about these two approaches to estimating statistics.

Note that, in the analytical developments below, we used biased but asymptotically unbiased estimates of the variance (i.e. the sum of squares is divided by the sample size without subtracting 1) which considerably simplifies the algebra in comparing the standard and block estimators. Because of the large sample sizes, the bias introduced is negligible, in particular in comparison with the difference we identify between standard and block estimators. To confirm this, the numerical results we provide use the unbiased estimators.

There is no difference between the two methods as far as the estimate $\hat{M}_{m,h}$ of the mean rainfall intensity for calendar month m and time-scale h is concerned:

$$\hat{M}_{m,h} = \frac{1}{N_y N_{m,h}} \sum_{j=1}^{j=N_y} \sum_{i=1}^{i=N_{m,h}} Y_{i,j,m}^{(h)}$$

where,

- N_y is the number of years,
- $N_{m,h}$ the number of time-steps at scale h in a month of calendar month m (for all months except February for which leap years would lead to a more complicated formula),
- $Y_{i,j,m}^{(h)}$ extends the notation introduced at the start of the paper: it is the rainfall depth in the i-th interval of the j-th month of calendar month m.

This is however no longer the case with the variance $V_{m,h}$ of the rainfall intensity for calendar month m and time-scale h for which the standard and block (biased) estimates are respectively:

$$\hat{V}^{[1]}_{m,h} = \frac{1}{N_y N_{m,h}} \sum_{j=1}^{j=N_y} \sum_{i=1}^{i=N_{m,h}} (Y^{(h)}_{i,j,m} - \hat{M}_{m,h})^2$$

$$\hat{V}^{[2]}_{m,h} = \frac{1}{N_y N_{m,h}} \sum_{j=1}^{j=N_y} \sum_{i=1}^{i=N_{m,h}} (Y^{(h)}_{i,j,m} - \overline{Y}^{(h)}_{j,m})^2$$

where, $\overline{Y}^{(h)}_{j,m} = \frac{\sum_{i=1}^{i=N_{m,h}} Y^{(h)}_{i,j,m}}{N_{m,h}}$ for $j = 1, ..., N_{m,h}$ are the the (sample) mean depths at time-scale h of the j-th month of calendar month m.

A little algebra shows a result that is also familiar from Analysis of variance (ANOVA), i.e. that the two estimators are related by:

$$\hat{V}^{[1]}_{m,h} = \hat{V}^{[2]}_{m,h} + V\hat{a}r(\overline{Y}^{(h)}_{j,m}) \tag{10}$$

where the added term is the (biased) sample variance of the above averages.

With the third-order centred moments, we also have two distinct expressions for their estimators:

$$\hat{T}^{[1]}_{m,h} = \frac{1}{N_y N_{m,h}} \sum_{j=1}^{j=N_y} \sum_{i=1}^{i=N_{m,h}} (Y^{(h)}_{i,j,m} - \hat{M}_{m,h})^3$$

$$\hat{T}^{[2]}_{m,h} = \frac{1}{N_y N_{m,h}} \sum_{j=1}^{j=N_y} \sum_{i=1}^{i=N_{m,h}} (Y^{(h)}_{i,j,m} - \overline{Y}^{(h)}_{j,m})^3$$

which are related by the following equation:

$$\hat{T}^{[1]}_{m,h} = \hat{T}^{[2]}_{m,h} + \hat{T}(\overline{Y}^{(h)}_{j,m}) + \frac{3}{N_y N_{m,h}} \sum_{j=1}^{j=N_y} (\overline{Y}^{(h)}_{j,m} - \hat{M}_{m,h}) \sum_{i=1}^{i=N_{m,h}} (Y^{(h)}_{i,j,m} - \overline{Y}^{(h)}_{j,m})^2 \tag{11}$$

where $\hat{T}$ is the third-order centred moment.

5.2 Are the estimators significantly different? A brief analytical and numerical investigation

5.2.1 Block estimation of moments

To estimate the differences between estimators, we can first look at simple examples of independent realisations in which we sample a number of zeroes that corresponds to what is realistic for the proportion dry p at the scale of interest and a simple distribution for the rainfall depths of non-zero rainfalls is assumed, e.g. a Gamma or Generalised Pareto (hereafter GP) (see Menabde and Sivapalan (2000), Montfort and V.Witter (1986)), assuming $N_y = 50$ and $N_{m,h} = 30 \times 24$ (for hourly data).

We found the differences to be less than 1% in the case of either the variances or third-order moments as the additive terms in the equations relating them were found to be very small, for all the relevant time-scales of interest (5 mins to 24 hrs). In the case of the variance, this can be seen by noting that, $\overline{Y}^{(h)}_{j,m}$ has a population variance that is that of the rainfall depths divided by $N_{m,h}$. So the sample variance $\overline{Y}_{j,m}^{(h)}$ is of the same order of magnitude as $\frac{1}{N_{m,h}}\hat{V}_{m,h}^{[1]}$ which means that the added term in Eq. (10) will be very small. Similar considerations apply to the added terms in Eq. (11).

We also checked that these two methods provide an unbiased estimation of the population second and third-order centred moments, i.e. $V = Var(X)$ and $M3 = E\big[(X - E(X))^3\big]$. These are easily obtained in terms of the corresponding moments ($V_{>0}$ and $M3_{>0}$) of the distribution of non-zero rainfalls (i.e. of a Gamma or GP distribution) using the following easily derivable relations (where M and $M_{>0}$ are the means of the full and the non-zero only distributions):

$$V = (1-p)\big(V_{>0} + pM_{>0}\big) \tag{12}$$

$$M3 = (1-p)\big(M3_{>0} + 3pM_{>0}V_{>0} + p(2p-1)M_{>0}^3\big) \tag{13}$$

5.2.2 Block estimation of ratios

However, some authors apply the block estimation approach, not to the moments themselves, but to their ratios, i.e. the coefficient of variation instead of the variance, and the coefficient of skewness instead of the third-order moment (e.g. Kaczmarska et al. (2014)). That means that the block estimator of such ratios is obtained by averaging the estimates of these ratios from the relevant block from each of the years in the data set.

Here, there are no interesting relations to derive between the estimators from the standard and block methods, so we move directly to the simple numerical testing introduced in Sect. 5.2. For $h = 1$, and a proportion of dry periods of 0.9, we fitted a Gamma and a generalised Pareto (GP) to the non-zero rainfalls at Greenwich (UK). This yielded a Gamma$(1.1629, 0.692)$ and a GPD$(0.1795, 0.654, 0)$ respectively (with the first providing a better fit), with the parameters given, in order as shape, scale and, for the GP, location.

By generating 100 samples of 50 years of hourly data, we find that there is a non-negligible difference between the two estimation methods. Focusing upon the skewnesses, we find 95% simulation bands of $[5.68, 6.65]$ and $[5.50, 6.15]$ for the Gamma samples, i.e. differences that are still small but no longer negligible (of the order of 4%).The block estimates clearly underestimate the population skewness of 6.40. Further, if we look at rainfall from a summer month, e.g. the month of August, these differences are more marked. For the Gamma distribution (Gamma$(0.848, 1.4)$) the bands are now $[6.48, 7.62]$ and $[6.26, 6.92]$ respectively, so a difference that is twice as large for the upper bounds. Again, the population skewness of 7.05 is underestimated by the block method.

When using the GP distribution (GPD$(0.1795, 0.654, 0)$), the differences between the two methods and the underestimation are starker. The bands are $[7.94, 13.97]$ and $[7.21, 8.55]$ for the standard and block method respectively. The latter underestimates the population skewness of 10.58 by quite a margin (these results are for the whole year; for August, the GP fit was poor and the population skewness infinite).

These results now need to be confirmed by looking at the case of a time-series with an appropriate correlation structure. This will enable us to ascertain to what extent introducing correlation impacts the performance of the estimators (which are, of course, theoretically designed for samples of independent realisations).

To do this, we use an RBL2 model calibrated to the same data used for the above sampling, namely Greenwich, UK. The idea is that this rainfall model provides us with a correlation structure that is close enough to the observed correlation to enable us to conclude as to how one would expect the block estimates to perform with such a correlation structure. We generate 100 samples of 50 years of hourly data with two sets of parameters, obtained from January (winter) and August (summer), respectively, and the associated theoretical skewnesses calculated from these two parameter sets are 7.69 and 21.73. The 95% simulation bands obtained from the sampled hourly time series are $[6.80, 7.65]$ and $[12.67, 14.65]$ using the block method, and $[7.11, 8.44]$ and $[16.70, 28.40]$ using the standard method. In line with the numerical investigation above, we find that, for both months, the theoretical skewnesses provided by the model equation are underestimated by the block estimate (the underestimation is particularly significant during summer month), while no significant deviation is obtained for the standard estimates.

The results we have obtained are indicative of a problem of underestimation of the skewness with the block estimation method, which is likely to have a significant impact upon the model's ability to reproduce the statistics of extreme rainfall.

6 Results and discussion

6.1 Block versus standard estimates

Models RBL1 and RBL2 are fitted using the original equations for these models. Although these equations are not shown in this paper, they are contained in the new sets of equations given above: for each statistic, the first equation given is that found in the past papers, with its domain of validity for α. We note that, for the RBL2, this is $\alpha > 1$ for all statistics, but we imposed $\alpha > 2$ for this model, in line with the work carried out by Kaczmarska et al. (2014). By using statistical estimators of the observed statistics based upon the standard and the block estimates as described in Sect. 5 (i.e. the block method takes averages of ratios), we define two different fitting methods, the standard (sM) and block (bM) fitting methods respectively.

Below, we consider:

- some standard theoretical statistics obtained when the two models are fitted with both methods and how these compare with the estimates derived from the observations using the standard and block methods;
- the extreme rainfall depths produced by simulating time-series of identical length to the observations; because of sampling variability, 250 simulations are carried out and the median is shown;
- the values of the parameters obtained in fitting these models with these two methods

While the mean rainfall depth (which has identical standard and block estimators) is nearly perfectly reproduced by both methods and models, Fig. 3 shows the differences in the skewness standard and block estimators (crosses and circles respectively).

Consequently, the models fitted to each also yield significantly different skewnesses. Since we know from the preliminary investigation in Sect. 5 that the standard estimator is much less biased, this means that the block fitting method significantly underestimates the skewness of the observations. This is an important conclusion with respect to the validity of previous work which has used the block fitting method.

We also note some interesting features of the two models' performance:

- good fits are obtained for RBL1 and RBL2 with the sM for all but the sub-hourly time-scales;
- at the finest time-scale under consideration (i.e. 5 and 10 mins for Bochum and Uccle respectively), there is a considerable underestimation of the skewness for bM and sM, in particular by the RBL1 model: this confirms the superiority of the RBL2 for fine time-scales noted by Kaczmarska et al. (2014)

While these results confirm the importance of using the standard estimation of observation statistics, this message is not as clear when we consider the reproduction of the coefficient of variation and autocorrelation lag-1, as Fig. 4 and Fig. 5 show. Due to space constraints, the examination of the effect of changing between bM and sM upon the variances at coarser time-scales will be presented together with the effect of using the new equations in Sect. 6.3.

From the figures above, we note that:

- the sub-hourly coefficients of variation estimated with the standard method are poorly reproduced by the sM as compared with the bM;
- the same is true of the sub-hourly and hourly autocorrelations

These results might seem a little surprising, so it is important to spell out exactly what they mean: the models fitted to the block estimates provide in some cases a better reproduction of the statistics than the models fitted to the standard estimates. This at the very least suggests that the improved reproduction of the skewness by the sM comes at the cost of other statistics being less well reproduced.

The benefit of an improved reproduction of the skewness upon the models' ability to reproduce the frequency of rainfall extremes at a range of scales is clear, as Fig. 6 shows.

Here, we observe

- sM significantly improves the reproduction of the extremes;
- RBL2 is superior to RBL1, in terms of reproducing the largest extremes in particular at the sub-hourly scales, but also, for instance at the daily scale

The importance of the reproduction of extreme values for the typical applications of such rainfall models means that even taking into account the problems with mean, coefficient of variation and autocorrelation, the sM is preferred. But this leaves us with an important question: are the shortcomings of the sM in reproducing some of these other statistics down to the model or the way it is fitted?

A clue to addressing this question can be obtained by looking at the parameters obtained when fitting with the sM method. Focusing for instance upon the RBL2, and recalling the constraint $\alpha > 2$, Table 1 shows that the model calibration has yielded values of α on the boundary (as in Kaczmarska et al. (2014)).

Recalling that α is the shape parameter of the distribution of η, a smaller α leads to a more skewed distribution for this parameter, and thereby also for those which scale with it, such as the storm mean cell intensity in the case of the RBL2. This enables the RBL2 to generate some much more intense cells and thereby yields higher values of the skewness of rainfall depths as we saw above, thereby explaining its superiority over the RBL1.

For model RBL1, the constraint upon α is defined by the limit of validity of the expression for the skewness (e.g. Onof et al. (2013)) i.e. $\alpha > 4$. The parameters that are obtained (Table 2) similarly show that the optimisation algorithm finds the optimum to be near this boundary for most month of the year.

For both models, the fact that the lower limit of parameter α is selected as optimal suggests that a re-examination of the domain of feasibility of the non-linear optimisation carried out when fitting the models is required. This is exactly what the use of the new equations allows us to do as we shall see below. Note that all the above results are confirmed by the Uccle data (see Sect. S2 in the Supplement).

6.2 New versus old equations

We now consider the performance of models RBL1 and RBL2 fitted using the new equations for these models presented in this paper. The impact of the use of these equations, if there is any, will be that of an extension of the domain of feasibility of parameter α. Since the results presented above have concluded to the superiority of the standard estimates of observation statistics, we shall use this method in what follows. As in the previous section, we examine (i) model parameters, (ii) the reproduction of standard statistics and (iii) the reproduction of extreme rainfall depth statistics.

Here it is useful to start with the parameters shown in Tables 3 and 4.

We see that, for most months, in the case of RBL1, and all but one month, in the case of RBL2, the optimal value of α was found outside the domain of feasibility imposed by the equations used in previous research, i.e. $\alpha > 4$ for RBL1 and $\alpha > 1$ for RBL2. For RBL1, we can check that for the months where the new values of α remain inside the old domain of feasibility, the optimal values of α are very similar to those in Table 2. That they are not identical is down to the randomness in the numerical tool used to optimise the objective function.

Looking now at the standard statistics, Figures 7-10 illustrate the impact of relaxing the constraint upon α in terms of the reproduction of the mean, coefficient of variation, autocorrelation lag-1 and skewness of the rainfall depths.

In these figures, aside from the theoretical estimates of the statistics, we show box plots of their sample estimates based upon 250 simulations of 5 minute (and 10 minute for Uccle, see Sect. S2 in Supplement) time-series of length equal to that of the observations (69 and 105 years for Bochum and Uccle, respectively). This is for two reasons. First it is important to check that the equations derived above are correct, which we can do by comparing estimates from these simulations with the theoretical values. Second, by including information about the simulation bands, we show the sampling variability which is useful to judge by how much a model statistic over- or under-estimates the corresponding observation statistic.

What the figures show very clearly is a general improvement of the reproduction of all these statistics, through the use of new equations. The broadening of parameter space thus enables the model to overcome the problem flagged earlier, namely that the attempt to reproduce fine-scale skewnesses led to a deterioration in the reproduction of the other depth statistics.

In particular, we want to draw the reader's attention to the RBL2's ability to reproduce the skewness at all scales of interest. This bodes well for its extreme-value performance which is shown in Fig. 11.

The improvement brought about by the broader parameter space is particular clear at the finest scale of interest (i.e. 5 and 10 minutes for Bochum and Uccle respectively). But we also note an improved reproduction of the extremes of lower return periods for sub-hourly and the hourly time-scale. These are however rather overestimated by both versions of the RBL2 model for coarser time-scales.

Without looking into the detail of the RBL1 model, the question of its performance as compared to the RBL2, with the new sets of equations in both cases, is illustrated in Fig. 12.

While noting that the above findings are broadly confirmed by the analysis of the Uccle data (see Sect. S2 in Supplement), we can conclude that RBL2 outperforms RBL1 for sub-hourly and hourly time-scales (the 20-min results at Uccle excepted). Aside from a somewhat better reproduction of low return period extremes by the RBL1 at the 6-hourly scale for Bochum, and since both models provide an equivalent satisfactory reproduction of the daily extreme rainfall depths (RBL2 is better for Uccle), RBL2 is therefore overall to be preferred for the reproduction of observed extremes.

6.3 Reproduction of coarse-scale variances

We briefly look at the impacts of the change of estimator of observational statistics and the use of the new equations upon the reproduction of coarse-scale variability.

Figure 13 shows that:

- as expected, the sM parameter estimates clearly outperform the bM estimates;
- unlike at finer time-scales, there is no clear improvement of the reproduction of the variance for daily-plus scales using new equations;
- beyond 7 days, many, and particularly the largest, of the variances are underestimated in line with the observations made by Marani (2003). This is even clearer in the case of the Uccle data (see Fig. S11 in Supplement)

This suggests that the issue of large-scale variability is probably best addressed by combining Poisson-cluster models with a coarse-scale model that constrain them so that large-scale variances are reproduced.

7 Conclusions

This paper has both corroborated certain observations made in previous studies and identified two important issues about how randomised Bartlett-Lewis models are fitted. In summary, first, the importance of the inclusion of the coefficient of skewness among the fitting properties (Cowpertwait, 1998) has indirectly been confirmed: it plays a key role in enabling a good reproduction of rainfall extremes. Second, the new randomised model (RBL2) introduced by Kaczmarska et al. (2014) has an overall better performance than the earlier version originally presented by Rodriguez-Iturbe et al. (1988), in particular in terms of its ability to reproduce extreme values and at . Third, we have shown that, while the weights used in the objective function require that estimates of the statistical properties used in the fitting be derived for each single month of the data set (to obtain their variance), in particular in the case of ratios such as the coefficients of variation or of skewness, these estimates should not be used to derive the overall estimates of the relevant statistical property. Rather, the estimates of rainfall statistics for each calendar month are best derived by pooling together all data from the relevant calendar month (with due attention to the separation between years in the case of the autocovariance) and using the standard sample statistics. Fourth, we have shown that the parameter spaces assumed in previous studies could be extended by relaxing the constraints imposed upon a parameter common to both randomised models (α). This improves in particular the RBL2 model's performance in reproducing both standard and extreme value statistics at sub-hourly and hourly time-scales. Fifth, the reproduction of coarse-scale variances (of a few days and more) is improved by using the standard method of estimating observation statistics, but the broader parameter space does not add much. As a result, we find that these Bartlett-Lewis models still tend rather to underestimate the variability at scales coarser than a week, which provides a confirmation of the wisdom of developing combinations of Bartlett-Lewis models with simple coarse-scale models to capture long-term variability (e.g. see Park et al. (2019) and forthcoming work).

Appendix A: Formulae for Fitting Properties

The complete formulae are given here for the selected statistical moments based upon different parameter ranges. These include mean, variance, lag-k auto-covariance and the third central moment of the discrete time aggregated process of the OBL, RBL1 and RBL2 models.

The definitions of the model parameters used are given below. When a parameter is only valid in some of the models, the models are indicated in square brackets:

- h: timescale
- λ: storm arrival rate
- η: cell duration parameter [OBL]
- α: shape parameter for the Gamma distribution of the cell duration parameter (η) [RBL1, RBL2]
- ν: scale parameter for the Gamma distribution of η [RBL1, RBL2]
- β: cell arrival rate [OBL]
- κ: ratio of the cell arrival rate to η (i.e. β/η)
- γ: storm termination rate [OBL]
- ϕ: ratio of the storm termination rate to η (i.e. γ/η)
- $\mu_X = E[X]$: mean cell intensity [OBL, RBL1]

– $\mu_{X^2} = E[X^2]$: mean of squares of cell intensities [OBL, RBL1]

– $\mu_{X^3} = E[X^3]$: mean of cubes of cell intensities [OBL, RBL1]

– ι: ratio of mean cell intensity to η (i.e. μ_X/η) [RBL2]

– $f_1 = \mu_{X^2}/\mu_X^2$

– $f_2 = \mu_{X^3}/\mu_X^3$

– $\mu_C = 1+\kappa/\phi$: mean number of cells per storm

A1 Bartlett-Lewis Rectangular Pulse Model (OBL)

Mean

$$M(h,\eta) = \frac{\lambda h \mu_x \mu_c}{\eta} \tag{A1}$$

Variance

$$\begin{aligned} V(h,\eta) \quad &= \quad 2\lambda\mu_c\mu_x^2 \left\{ \left(f_1 + \frac{\kappa}{\phi}\right)\frac{h}{\eta^2} + \left(\frac{\kappa}{\phi^2(\phi^2-1)}\right)\frac{1-e^{-\phi\eta h}}{\eta^3} \right. \\ &\left. + \left(f_1 + \frac{\kappa\phi}{\phi^2-1}\right)\frac{1-e^{-\eta h}}{\eta^3} \right\} \end{aligned} \tag{A2}$$

Covariance at lag $k \geq 1$

$$\begin{aligned} C(k,h) \quad &= \quad \frac{\lambda\mu_c\mu_x^2}{\eta^3} \left\{ \left(f_1 + \frac{\kappa\phi}{\phi^2-1}\right)\left[e^{-\eta(k-1)h} - 2e^{-\eta kh} + e^{-\eta(k+1)h}\right] \right. \\ &\left. - \left(\frac{\kappa}{\phi^2(\phi^2-1)}\right)\left[e^{-\eta\phi(k-1)h} - 2e^{-\eta\phi kh} + e^{-\eta\phi(k+1)h}\right] \right\} \end{aligned} \tag{A3}$$

Third central moment

$$S(h,\eta) = E\left[\left(Y_i^{(h)} - E(Y_i^h)\right)^3\right] = \frac{\lambda\mu_c\mu_x^3 \sum_{k=1}^{k=8} P_k(\phi,\kappa,\eta,f_1,f_2)}{(1+2\phi+\phi^2)(\phi^4-2\phi^3-3\phi^2+8\phi-4)\phi^3} \tag{A4}$$

where the quantities $P_k\{\phi,\kappa,\eta,f_1,f_2\}$ are given by the following equations:

$$
\begin{aligned}
P_1(\phi,\kappa,\eta,f_1,f_2) &= 6\eta^{-4}e^{-\eta h}\phi^2\left[\phi\kappa^2(2\phi^4-7\phi^2-3\phi+2)+2\phi f_2(\phi^6-6\phi^4+9\phi^2-4)\right.\\
&\quad \left.+\kappa f_1(4\phi^6-22\phi^4-\phi^3+25\phi^2+4\phi-4)\right]\\
P_2(\phi,\kappa,\eta,f_1,f_2) &= 6\eta^{-3}e^{-\eta h}\phi^3 h\left[f_2(\phi^6-6\phi^4+9\phi^2-4)+\phi\kappa f_1(\phi^2-1)(\phi^2-4)\right]\\
P_3(\phi,\kappa,\eta,f_1,f_2) &= 6\eta^{-4}e^{-\eta\phi h}\kappa\left[f_1(-\phi^5+\phi^4+6\phi^3-4\phi^2-8\phi)\right.\\
&\quad \left.+\kappa(\phi^5-3\phi^4+2\phi^3+14\phi^2-8)\right]\\
P_4(\phi,\kappa,\eta,f_1,f_2) &= 6\eta^{-3}e^{-\eta\phi h}h\kappa^2\left[\phi^3(5-\phi^2)-4\phi\right]\\
P_5(\phi,\kappa,\eta,f_1,f_2) &= \eta^{-4}\left[-12\phi^3 f_2(\phi^6-6\phi^4+9\phi^2-4)\right.\\
&\quad +\kappa^2(-9\phi^7+39\phi^5+18\phi^4-12\phi^3-84\phi^2+48)\\
&\quad \left.-3\phi\kappa f_1(7\phi^7-39\phi^5-2\phi^4+46\phi^3+12\phi^2-8\phi-16)\right]\\
P_6(\phi,\kappa,\eta,f_1,f_2) &= \eta^{-3}\left[(6h\phi^3 f_2+12h\phi^2\kappa f_1+6h\phi\kappa^2)(\phi^6-6\phi^4+9\phi^2-4)\right]\\
P_7(\phi,\kappa,\eta,f_1,f_2) &= 3\eta^{-4}e^{-2\eta h}\phi^4(1-\phi^2)\left[\phi\kappa^2+\kappa f_1(\phi^2-4)\right]\\
P_8(\phi,\kappa,\eta,f_1,f_2) &= 6\eta^{-4}e^{-(1+\phi)\eta h}\kappa\phi^2(\phi-2)(\phi-1)\left[f_1(\phi+2)-\phi\kappa\right]
\end{aligned}
$$

A2 Randomised Bartlett-Lewis Rectangular Pulse Model (RBL1)

Mean

$$M(h)=\frac{\lambda h\mu_x\mu_c\nu}{\alpha-1} \tag{A5}$$

Variance

$$
\begin{aligned}
V(h) &= 2\lambda\mu_c\mu_x^2\left[\left(f_1+\frac{\kappa}{\phi}\right)hT(2,0,0)+\left(\frac{\kappa(1-\phi^3)}{\phi^2(\phi^2-1)}-f_1\right)T(3,0,0)\right.\\
&\quad \left.-\frac{\kappa}{\phi^2(\phi^2-1)}T(3,\phi h,0)+\left(f_1+\frac{\kappa\phi}{\phi^2-1}\right)T(3,h,0)\right]\\
&\quad \text{for } \alpha>3\\
V(h) &\approx 2\lambda\mu_c\mu_x^2\left[\frac{\nu^\alpha h^2\eta_0^{\alpha-1}}{2(\alpha-1)\Gamma(\alpha)}\left(\frac{\kappa}{\phi+1}+f_1\right)\right.\\
&\quad +\left(f_1+\frac{\kappa}{\phi}\right)hT(2,0,\eta_0)+\left(\frac{\kappa(1-\phi^3)}{\phi^2(\phi^2-1)}-f_1\right)T(3,0,\eta_0)\\
&\quad \left.-\left(\frac{\kappa}{\phi^2(\phi^2-1)}\right)T(3,\phi h,\eta_0)+\left(f_1+\frac{\kappa\phi}{\phi^2-1}\right)T(3,h,\eta_0)\right]\\
&\quad \text{for } 1<\alpha\leq 3\\
V(h) &= \infty\\
&\quad \text{for } \alpha\leq 1
\end{aligned}
\tag{A6}
$$

Covariance at lag $k \geq 1$

$$
\begin{aligned}
C(k,h) &= \lambda\mu_c\mu_x^2\left\{\left(f_1+\frac{\kappa\phi}{\phi^2-1}\right)[T(3,(k-1)h,0)-2T(3,kh,0)+T(3,(k+1)h,0)]\right.\\
&\quad \left.-\left(\frac{\kappa}{\phi^2(\phi^2-1)}\right)[T(3,\phi(k-1)h,0)-2T(3,\phi kh,0)+T(3,\phi(k+1)h,0)]\right\}\\
&\quad \text{for } \alpha>3\\
C(k,h) &\approx \lambda\mu_c\mu_x^2\left\{\frac{\nu^\alpha h^2\eta_0^{\alpha-1}}{(\alpha-1)\Gamma(\alpha)}\left(\frac{\kappa}{\phi+1}+f_1\right)\right.\\
&\quad +\left(f_1+\frac{\kappa\phi}{\phi^2-1}\right)[T(3,(k-1)h,\eta_0)-2T(3,kh,\eta_0)+T(3,(k+1)h,\eta_0)]\\
&\quad \left.-\left(\frac{\kappa}{\phi^2(\phi^2-1)}\right)[T(3,\phi(k-1)h,\eta_0)-2T(3,\phi kh,\eta_0,)+T(3,\phi(k+1)h,\eta_0,)]\right\}\\
&\quad \text{for } 1<\alpha\leq 3\\
C(k,h) &= \infty\\
&\quad \text{for } \alpha\leq 1
\end{aligned}
\tag{A7}
$$

Third central moment

$$
\begin{aligned}
S(h) &= \frac{\lambda\mu_c\mu_x^3\sum_{k=1}^{k=8}Q_k\left(\phi,\kappa,f_1,f_2,0\right)}{(1+2\phi+\phi^2)(\phi^4-2\phi^3-3\phi^2+8\phi-4)\phi^3}\\
&\quad \text{for } \alpha>4\\
S(h) &\approx \frac{\lambda\mu_c\mu_x^3}{(1+2\phi+\phi^2)(\phi^4-2\phi^3-3\phi^2+8\phi-4)\phi^3}\\
&\quad \left[\frac{\nu^\alpha\eta_0^{\alpha-1}h^3}{\Gamma(\alpha)(\alpha-1)}\left(2\kappa^2(\phi^7-3\phi^6+\phi^5+3\phi^4-2\phi^3)+f_2(\phi^9-6\phi^7+9\phi^5-4\phi^3)\right.\right.\\
&\quad \left.+3\kappa f_1(\phi^8-\phi^7-5\phi^6+5\phi^5+4\phi^4-4\phi^3)\right)\\
&\quad \left.+\sum_{k=1}^{k=8}Q_k\left(\phi,\kappa,f_1,f_2,\eta_0\right)\right]\\
&\quad \text{for } 1<\alpha\leq 4\\
S(h) &= \infty\\
&\quad \text{for } \alpha\leq 1
\end{aligned}
\tag{A8}
$$

and the quantities $Q_k\{\phi,\kappa,f_1,f_2,l\}$ are given by the following equations:

$$
\begin{aligned}
Q_1(\phi,\kappa,f_1,f_2,l) &= 6T(4,h,l)\phi^2\left[\phi\kappa^2(2\phi^4-7\phi^2-3\phi+2)+2\phi f_2(\phi^6-6\phi^4+9\phi^2-4)\right.\\
&\quad\left.+\kappa f_1(4\phi^6-22\phi^4-\phi^3+25\phi^2+4\phi-4)\right]\\
Q_2(\phi,\kappa,f_1,f_2,l) &= 6T(3,h,l)\phi^3 h\left[f_2(\phi^6-6\phi^4+9\phi^2-4)+\phi\kappa f_1(\phi^2-1)(\phi^2-4)\right]\\
Q_3(\phi,\kappa,f_1,f_2,l) &= 6T(4,\phi h,l)\kappa\left[f_1(-\phi^5+\phi^4+6\phi^3-4\phi^2-8\phi)\right.\\
&\quad\left.+\kappa(\phi^5-3\phi^4+2\phi^3+14\phi^2-8)\right]\\
Q_4(\phi,\kappa,f_1,f_2,l) &= 6T(3,\phi h,l)\kappa^2 h\left[\phi^3(5-\phi^2)-4\phi\right]\\
Q_5(\phi,\kappa,f_1,f_2,l) &= T(4,0,l)\left[-12\phi^3 f_2(\phi^6-6\phi^4+9\phi^2-4)\right.\\
&\quad+\kappa^2(-9\phi^7+39\phi^5+18\phi^4-12\phi^3-84\phi^2+48)\\
&\quad\left.-3\phi\kappa f_1(7\phi^7-39\phi^5-2\phi^4+46\phi^3+12\phi^2-8\phi-16)\right]\\
Q_6(\phi,\kappa,f_1,f_2,l) &= T(3,0,l)\left[(6h\phi^3 f_2+12h\phi^2\kappa f_1+6h\phi\kappa^2)(\phi^6-6\phi^4+9\phi^2-4)\right]\\
Q_7(\phi,\kappa,f_1,f_2,l) &= 3T(4,2h,l)\phi^4(1-\phi^2)\left[\phi\kappa^2+\kappa f_1(\phi^2-4)\right]\\
Q_8(\phi,\kappa,f_1,f_2,l) &= 6T(4,(1+\phi)h,l)\kappa\phi^2(\phi-2)(\phi-1)\left[f_1(\phi+2)-\phi\kappa\right]
\end{aligned}
$$

A3 Randomised Parameter Bartlett-Lewis Rectangular Pulse Model with Dependent Intensity-Duration (RBL2)

Mean

$$M(h)=\lambda h\iota\mu_c \tag{A9}$$

Variance

$$
\begin{aligned}
V(h) &= 2\lambda\mu_c\iota^2\left[\left(f_1+\frac{\kappa}{\phi}\right)h+\left(\frac{\kappa(1-\phi^3)}{\phi^2(\phi^2-1)}-f_1\right)T(1,0,0)\right.\\
&\quad\left.-\left(\frac{\kappa}{\phi^2(\phi^2-1)}\right)T(1,\phi h,0)+\left(f_1+\frac{\kappa\phi}{\phi^2-1}\right)T(1,h,0)\right]\\
&\quad\text{for } \alpha>1\\
V(h) &\approx 2\lambda\mu_c\iota^2\left[\frac{\eta_0^{\alpha+1}h^2\nu^\alpha}{2(\alpha+1)\Gamma(\alpha)}\left(\frac{\kappa}{\phi+1}+f_1\right)\right.\\
&\quad+\left(f_1+\frac{\kappa}{\phi}\right)hT(0,0,\eta_0)+\left(\frac{\kappa(1-\phi^3)}{\phi^2(\phi^2-1)}-f_1\right)T(1,0,\eta_0)\\
&\quad\left.-\left(\frac{\kappa}{\phi^2(\phi^2-1)}\right)T(1,\phi h,\eta_0)+\left(f_1+\frac{\kappa\phi}{\phi^2-1}\right)T(1,h,\eta_0)\right]\\
&\quad\text{for } -1<\alpha\le 1
\end{aligned}
\tag{A10}
$$

Covariance at lag $k \geq 1$

$$
\begin{aligned}
C(k,h) &= \lambda\mu_c\iota^2\left\{\left(f_1+\frac{\kappa\phi}{\phi^2-1}\right)[T(1,(k-1)h,0)-2T(1,kh,0)+T(1,(k+1)h,0)]\right.\\
&\quad\left.-\left(\frac{\kappa}{\phi^2(\phi^2-1)}\right)[T(1,\phi(k-1)h,0)-2T(1,\phi kh,0)+T(1,\phi(k+1)h,0)]\right\}\\
&\quad \text{for } \alpha>1\\
C(k,h) &\approx \lambda\mu_c\iota^2\left\{\frac{\eta_0^{\alpha+1}h^2\nu^\alpha}{\Gamma(\alpha)(\alpha+1)}\left(f_1+\frac{\kappa}{\phi+1}\right)\right.\\
&\quad+\left(f_1+\frac{\kappa\phi}{\phi^2-1}\right)[T(1,(k-1)h,\eta_0)-2T(1,kh,\eta_0)+T(1,(k+1)h,\eta_0)]\\
&\quad\left.-\left(\frac{\kappa}{\phi^2(\phi^2-1)}\right)[T(1,\phi(k-1)h,\eta_0)-2T(1,\phi kh,\eta_0)+T(1,\phi(k+1)h,\eta_0)]\right\}\\
&\quad \text{for } -1<\alpha\leq 1
\end{aligned}
\tag{A11}
$$

Third central moment

$$
\begin{aligned}
S(h) &= \frac{\lambda\mu_c\iota^3\sum_{k=1}^{k=8}P_k(\phi,\kappa,f_1,f_2,0)}{(1+2\phi+\phi^2)(\phi^4-2\phi^3-3\phi^2+8\phi-4)\phi^3}\\
&\quad \text{for } \alpha>1\\
S(h) &\approx \frac{\lambda\mu_c\iota^3}{(1+2\phi+\phi^2)(\phi^4-2\phi^3-3\phi^2+8\phi-4)\phi^3}\\
&\quad\left[\frac{\nu^\alpha\eta_0^{\alpha+2}h^3}{\Gamma(\alpha)(\alpha+2)}\big(2\kappa^2(\phi^7-3\phi^6+\phi^5+3\phi^4-2\phi^3)+f_2(\phi^9-6\phi^7+9\phi^5-4\phi^3)\right.\\
&\quad+3\kappa f_1(\phi^8-\phi^7-5\phi^6+5\phi^5+4\phi^4-4\phi^3)\big)\\
&\quad\left.+\sum_{k=1}^{k=8}P_k(\phi,\kappa,f_1,f_2,\eta_0)\right]\\
&\quad \text{for } -2<\alpha\leq 1
\end{aligned}
\tag{A12}
$$

with:

$$\begin{aligned}
P_1(\phi,\kappa,f_1,f_2,l) &= 6T(1,h,l)\phi^2\left[\phi\kappa^2(2\phi^4-7\phi^2-3\phi+2)+2\phi f_2(\phi^6-6\phi^4+9\phi^2-4)\right.\\
&\quad\left.+\kappa f_1(4\phi^6-22\phi^4-\phi^3+25\phi^2+4\phi-4)\right]\\
P_2(\phi,\kappa,f_1,f_2,l) &= 6T(0,h,l)\phi^3 h\left[f_2(\phi^6-6\phi^4+9\phi^2-4)+\phi\kappa f_1(\phi^2-1)(\phi^2-4)\right]\\
P_3(\phi,\kappa,f_1,f_2,l) &= 6T(1,\phi h,l)\kappa\left[f_1(-\phi^5+\phi^4+6\phi^3-4\phi^2-8\phi)\right.\\
&\quad\left.+\kappa(\phi^5-3\phi^4+2\phi^3+14\phi^2-8)\right]\\
P_4(\phi,\kappa,f_1,f_2,l) &= 6T(0,\phi h,l)h\kappa^2\left[\phi^3(5-\phi^2)-4\phi\right]\\
P_5(\phi,\kappa,f_1,f_2,l) &= T(1,0,l)\left[-12\phi^3 f_2(\phi^6-6\phi^4+9\phi^2-4)\right.\\
&\quad+\kappa^2(-9\phi^7+39\phi^5+18\phi^4-12\phi^3-84\phi^2+48)\\
&\quad\left.-3\phi\kappa f_1(7\phi^7-39\phi^5-2\phi^4+46\phi^3+12\phi^2-8\phi-16)\right]\\
P_6(\phi,\kappa,f_1,f_2,l) &= T(0,0,l)\left[(6h\phi^3 f_2+12h\phi^2\kappa f_1+6h\phi\kappa^2)(\phi^6-6\phi^4+9\phi^2-4)\right]\\
P_7(\phi,\kappa,f_1,f_2,l) &= 3T(1,2h,l)\phi^4(1-\phi^2)\iota^3\left[\phi\kappa^2+\kappa f_1(\phi^2-4)\right]\\
P_8(\phi,\kappa,f_1,f_2,l) &= 6T(1,(1+\phi)h,l)\kappa\phi^2(\phi-2)(\phi-1)\iota^3\left[f_1(\phi+2)-\phi\kappa\right]
\end{aligned}$$

Appendix B: Relation between cell intensity parameters

In the model equations, parameters μ_x, f_1 and f_2 for the RBL1 and ι, f_1 and f_2 for the RBL2 are three unrelated model parameters only if a three-parameter distribution is chosen for the cell intensity. If a two-parameter distribution is chosen, there will effectively be two unrelated parameters, if a one-parameter distribution is chosen, there will only be one.

Starting with the last case first, the standard choice is the exponential distribution:

$$f_X(x) = ae^{-ax} \text{ for } x > 0$$

for which:

$$\begin{aligned}
\mu_x &= 1/a\\
f_1 &= 2\\
f_2 &= 6
\end{aligned}$$

So, for the exponential distribution, the only free parameter is μ_x for the RBL1 and ι for the RBL2.

Next, we can seek to have more flexibility by using the Gamma distribution:

$$f_X(x) = \frac{x^{a-1}e^{-x/b}}{b^a\Gamma(a)} \text{ for } x > 0$$

for which:

$$\begin{aligned}
\mu_x &= ab \\
f_1 &= \frac{a+1}{a} \\
f_2 &= \frac{a^2+3a+2}{a^2}
\end{aligned}$$

So, for the Gamma distribution there would be two free parameters μ_x or ι, and f_1, with f_2 obtained as the following function of f_1:

$$f_2 = 2f_1^2 - f_1$$

The Pareto distribution is a thick-tailed distribution that will produce larger extremes:

$$f_X(x) = \frac{ab^a}{x^{a+1}} \text{ for } x \geq b$$

and for this distribution, we have:

$$\begin{aligned}
\mu_x &= \frac{ab}{a-1} \qquad (\text{if } a > 1) \\
f_1 &= \frac{(a-1)^2}{a(a-2)} \qquad (\text{if } a > 2 \text{ i.e. } f_1 > 1) \\
f_2 &= \frac{(a-1)^3}{a^2(a-3)} \qquad (\text{if } a > 3 \text{ i.e. } f_2 > 1)
\end{aligned}$$

For the Pareto distribution there would also be two free parameters μ_x or ι, and f_1, with $f_2$obtained as the following function of f_1:

$$f_2 = \frac{f_1^{3/2}}{f_1^{1/2}(3-2f_1) - 2(f_1-1)^{3/2}}$$

where we have to have $f_1 < 4/3$ to fulfill the condition $a > 3$.

Finally, a mixed distribution could be chosen, e.g. one which is a mixture of Gamma and Pareto, with weight ω representing the probability of sampling from a Gamma rather than a Pareto. This would be defined by the following pdf:

$$f_X(x) = \omega \frac{x^{a-1}e^{-x/b}}{b^a\Gamma(a)} + (1-\omega)\frac{cd^c}{x^{c+1}} \text{ for } x \geq d$$

for which the moments are just weighted combinations of those of the Gamma and Pareto distributions:

$$\begin{aligned}
\mu_x &= \omega ab + (1-\omega)\frac{cd}{c-1} \qquad (\text{if } c > 1) \\
f_1 &= \frac{\omega(a+1)ab^2 + (1-\omega)\frac{cd^2}{c-2}}{\left(\omega ab + (1-\omega)\frac{cd}{c-1}\right)^2} \qquad (\text{if } c > 2) \\
f_2 &= \frac{\omega(a^2+3a+2)ab^3 + (1-\omega)\frac{cd^3}{c-3}}{\left(\omega ab + (1-\omega)\frac{cd}{c-1}\right)^3} \qquad (\text{if } c > 3)
\end{aligned}$$

Here, we would have three free parameters, μ_x, f_1 and f_2 and for the purposes of simulation, we would seek parameters ω, a, b, c and d for which the three right-hand sides of the above equations would be equal to μ_x, f_1 and f_2, for instance by minimising a sum of squares. This optimisation problem is underdetermined, but it would make sense to choose at least for the Gamma parameters a and b, values close to values obtained when fitting a Gamma distribution as starting values, or indeed to fix these two parameters to these values.

Appendix C: Example of integral divergence

The integral of a sum of terms is only equal to the sum of the integrals of each additive term when the latter are finite. When the latter are infinite, this is not necessarily the case. That is, it is possible that the integral of the sum should be finite while the integrals of the additive terms are infinite. This appendix shows an example to illustrate this.

Consider the following integrals:

$$\begin{aligned} I(x) &= \int_0^x \frac{e^{\omega t} - e^{-\sigma t}}{t} dt \\ I_1(x) &= \int_0^x \frac{e^{\omega t}}{t} dt \\ I_2(x) &= \int_0^x -\frac{e^{-\sigma t}}{t} dt \end{aligned}$$

The integrals $I_1(x)$ and $I_2(x)$ are divergent integrals because the integrands behave as $1/t$ and $-1/t$ respectively, in the vicinity of 0. So $I_1(x) = +\infty$ and $I_2(x) = -\infty$.

However, using Taylor expansions, we can see that $I(x)$ is finite:

$$\begin{aligned} I(x) &= \int_0^x \frac{1 + \omega t - 1 + \sigma t + o(t)}{/} t dt \\ &= \int_0^x (\omega + \sigma + o(1)) dt \end{aligned}$$

Therefore:

$$I(x) = (\omega + \sigma)x + o(x)$$

and

$$I(x) \neq I_1(x) + I_2(x)$$

Author contributions. CO and LW conceptulised the research idea and designed the experiment. CO derived new equations. LW validated the equations and implemented code and performed the simulations. CO prepared the manuscript with contributions from LW.

Competing interests. The authors declare that they have no conflict of interest.

Acknowledgements. The authors are grateful for the financial support provided by the Era-Net FloodCitiSense project. The authors would also like to thank Deutsche Montan Technologie and the Emschergenossenschaft/Lippeverband for providing Bochum rainfall data, and the Royal Meteorological Institute of Belgium for providing Uccle rainfall data.

References

Arnbjerg-Nielsen, K.: Quantification of climate change effects on extreme precipitation used for high resolution hydrologic design, Urban Water Journal, 9, 57–65, https://doi.org/10.1080/1573062X.2011.630091, https://doi.org/10.1080/1573062X.2011.630091, 2012.

Arnbjerg-Nielsen, K., Willems, P., Olsson, J., Beecham, S., Pathirana, A., Bülow Gregersen, I., Madsen, H., and Nguyen, V.-T.-V.: Impacts of climate change on rainfall extremes and urban drainage systems: a review, Water Science and Technology, 68, 16–28, https://doi.org/10.2166/wst.2013.251, https://doi.org/10.2166/wst.2013.251, 2013.

Burlando, P. and Rosso, R.: Stochastic Models of Temporal Rainfall: Reproducibility, Estimation and Prediction of Extreme Events, in: Stochastic Hydrology and its Use in Water Resources Systems Simulation and Optimization, edited by Marco, J. B., Harboe, R., and Salas, J. D., pp. 137–173, Springer Netherlands, Dordrecht, https://doi.org/10.1007/978-94-011-1697-8_7, https://doi.org/10.1007/978-94-011-1697-8_7, 1993.

Connolly, R., Schirmer, J., and Dunn, P.: A daily rainfall disaggregation model, Agricultural and Forest Meteorology, 92, 105 – 117, https://doi.org/10.1016/S0168-1923(98)00088-4, http://www.sciencedirect.com/science/article/pii/S0168192398000884, 1998.

Cowpertwait, P. S. P.: A Poisson-cluster model of rainfall: some high-order moments and extreme values, Proceedings of the Royal Society of London A: Mathematical, Physical and Engineering Sciences, 454, 885–898, https://doi.org/10.1098/rspa.1998.0191, http://rspa.royalsocietypublishing.org/content/454/1971/885, 1998.

Cross, D., Onof, C., and Winter, H.: Ensemble simulation of future rainfall extremes with temperature dependent censored simulation, Advances in Meteorology, 2019.

Efstratiadis, A., Koutsoyiannis, D., and Polytechniou, H.: An evolutionary annealing-simplex algorithm for global optimisation of water resource systems, in: Hydroinformatics 2002: Proceedings of the Fifth International Conference on Hydroinformatics, International Water Association, 2002.

Evin, G. and Favre, A.-C.: A new rainfall model based on the Neyman-Scott process using cubic copulas, Water Resources Research, 44, W03 433, https://doi.org/10.1029/2007WR006054, https://agupubs.onlinelibrary.wiley.com/doi/abs/10.1029/2007WR006054, 2008.

Jesus, J. and Chandler, R. E.: Estimating functions and the generalized method of moments, Interface Focus, 1, 871–885, https://doi.org/10.1098/rsfs.2011.0057, http://rsfs.royalsocietypublishing.org/content/1/6/871, 2011.

Kaczmarska, J., Isham, V., and Onof, C.: Point process models for fine-resolution rainfall, Hydrological Sciences Journal, 59, 1972–1991, https://doi.org/10.1080/02626667.2014.925558, https://doi.org/10.1080/02626667.2014.925558, 2014.

Kaczmarska, J. M., Isham, V. S., and Northrop, P.: Local generalised method of moments: an application to point process-based rainfall models, Environmetrics, 26, 312–325, https://doi.org/10.1002/env.2338, 2015.

Khaliq, M. and Cunnane, C.: Modelling point rainfall occurrences with the modified Bartlett-Lewis rectangular pulses model, Journal of Hydrology, 180, 109 – 138, https://doi.org/https://doi.org/10.1016/0022-1694(95)02894-3, http://www.sciencedirect.com/science/article/pii/0022169495028943, 1996.

Kim, J.-G., Kwon, H.-H., and Kim, D.: A hierarchical Bayesian approach to the modied Bartlett-Lewis rectangular pulse model for a joint estimation of model parameters across stations, Journal of Hydrology, 544, 210–223, https://doi.org//10.1016/j.jhydrol.2016.11.031, http://www.sciencedirect.com/science/article/pii/S0022169416307375, 2017.

Kossieris, P., Makropoulos, C., Onof, C., and Koutsoyiannis, D.: A rainfall disaggregation scheme for sub-hourly time scales: Coupling a Bartlett-Lewis based model with adjusting procedures, Journal of Hydrology, 556, 980 – 992, https://doi.org/10.1016/j.jhydrol.2016.07.015, http://www.sciencedirect.com/science/article/pii/S0022169416304450, 2018.

Koutsoyiannis, D. and Mamassis, N.: On the representation of hyetograph characteristics by stochastic rainfall models, Journal of Hydrology, 251, 65 – 87, https://doi.org//10.1016/S0022-1694(01)00441-3, http://www.sciencedirect.com/science/article/pii/S0022169401004413, 2001.

Marani, M.: On the correlation structure of continuous and discrete point rainfall, Water Resources Research, 39, 1128, https://doi.org/10.1029/2002WR001456, https://agupubs.onlinelibrary.wiley.com/doi/abs/10.1029/2002WR001456, 2003.

Menabde, M. and Sivapalan, M.: Modeling of rainfall time series and extremes using bounded random cascades and levy-stable distributions, Water Resources Research, 36, 3293–3300, https://doi.org/10.1029/2000WR900197, https://agupubs.onlinelibrary.wiley.com/doi/abs/10.1029/2000WR900197, 2000.

Montfort, M. A. and V.Witter, J.: The Generalized Pareto distribution applied to rainfall depths, Hydrological Sciences Journal, 31, 151–162, https://doi.org/10.1080/02626668609491037, https://doi.org/10.1080/02626668609491037, 1986.

Onof, C. and Arnbjerg-Nielsen, K.: Quantification of anticipated future changes in high resolution design rainfall for urban areas, Atmospheric Research, 92, 350 – 363, https://doi.org/10.1016/j.atmosres.2009.01.014, http://www.sciencedirect.com/science/article/pii/S0169809509000313, 7th International Workshop on Precipitation in Urban Areas, 2009.

Onof, C. and Wheater, H. S.: Modelling of British rainfall using a random parameter Bartlett-Lewis Rectangular Pulse Model, Journal of Hydrology, 149, 67 – 95, https://doi.org/10.1016/0022-1694(93)90100-N, http://www.sciencedirect.com/science/article/pii/002216949390100N, conventry Groundwater Investigation: Sources and Movement of Chlorinated Hydrocarbon Solvents, 1993.

Onof, C. and Wheater, H. S.: Improvements to the modelling of British rainfall using a modified Random Parameter Bartlett-Lewis Rectangular Pulse Model, Journal of Hydrology, 157, 177 – 195, https://doi.org/10.1016/0022-1694(94)90104-X, http://www.sciencedirect.com/science/article/pii/002216949490104X, 1994.

Onof, C., Chandler, R. E., Kakou, A., Northrop, P., Wheater, H. S., and Isham, V.: Rainfall modelling using Poisson-cluster processes: a review of developments, Stochastic Environmental Research and Risk Assessment, 14, 384–411, https://doi.org/10.1007/s004770000043, https://doi.org/10.1007/s004770000043, 2000.

Onof, C., Meca-Figueras, T., Kaczmarska, J., Chandler, R., and Hege, L.: Modelling rainfall with a Bartlett–Lewis process: third order moments, proportion dry, and a truncated random parameter version, Tech. rep., Imperial College London, 2013.

Park, J., Onof, C., and Kim, D.: A hybrid stochastic rainfall model that reproduces some important rainfall characteristics at hourly to yearly timescales, Hydrology and Earth System Sciences, 23, 989–1014, https://doi.org/10.5194/hess-23-989-2019, http://dx.doi.org/10.5194/hess-23-989-2019, 2019.

Paschalis, A., Molnar, P., Fatichi, S., and Burlando, P.: On temporal stochastic modeling of precipitation, nesting models across scales, Advances in Water Resources, 63, 152 – 166, https://doi.org/10.1016/j.advwatres.2013.11.006, http://www.sciencedirect.com/science/article/pii/S0309170813002376, 2014.

Ramesh, N. I.: Statistical analysis on Markov-modulated Poisson processes, Environmetrics, 6, 165–179, https://doi.org/10.1002/env.3170060207, https://onlinelibrary.wiley.com/doi/abs/10.1002/env.3170060207, 1995.

Ramesh, N. I., Garthwaite, A. P., and Onof, C.: A doubly stochastic rainfall model with exponentially decaying pulses, Stochastic Environmental Research and Risk Assessment, 32, 1645–1664, https://doi.org/10.1007/s00477-017-1483-z, https://doi.org/10.1007/s00477-017-1483-z, 2018.

Rodriguez-Iturbe, I., Cox, D. R., and Isham, V.: Some models for rainfall based on stochastic point processes, Proceedings of the Royal Society of London A: Mathematical, Physical and Engineering Sciences, 410, 269–288, https://doi.org/10.1098/rspa.1987.0039, http://rspa.royalsocietypublishing.org/content/410/1839/269, 1987.

Rodriguez-Iturbe, I., Cox, D. R., and Isham, V.: A point process model for rainfall: further developments, Proceedings of the Royal Society of London A: Mathematical, Physical and Engineering Sciences, 417, 283–298, https://doi.org/10.1098/rspa.1988.0061, http://rspa.royalsocietypublishing.org/content/417/1853/283, 1988.

Verhoest, N., Troch, P. A., and Troch, F. P. D.: On the applicability of Bartlett–Lewis rectangular pulses models in the modeling of design storms at a point, Journal of Hydrology, 202, 108 – 120, https://doi.org/10.1016/S0022-1694(97)00060-7, http://www.sciencedirect.com/science/article/pii/S0022169497000607, 1997.

Verhoest, N. E. C., Vandenberghe, S., Cabus, P., Onof, C., Meca-Figueras, T., and Jameleddine, S.: Are stochastic point rainfall models able to preserve extreme flood statistics?, Hydrological Processes, 24, 3439–3445, https://doi.org/10.1002/hyp.7867, https://onlinelibrary.wiley.com/doi/abs/10.1002/hyp.7867, 2010.

Wang, L., Onof, C., and Maksimovic, C.: Reconstruction of sub-daily rainfall sequences using multinomial multiplicative cascades, Hydrology and Earth System Sciences Discussions, 7, 5267–5297, https://doi.org/10.5194/hessd-7-5267-2010, https://www.hydrol-earth-syst-sci-discuss.net/7/5267/2010/, 2010.

Wheater, H. S., Isham, V. S., Chandler, R. E., Onof, C., Bellone, E., Prudhomme, C., and Crooks, S.: Improved methods for national spatial-temporal rainfall and evaporation modelling for BSM, Tech. rep., DEFRA, randd.defra.gov.uk/Document.aspx?Document=FD2105_6227_PR.pdf, 2006.

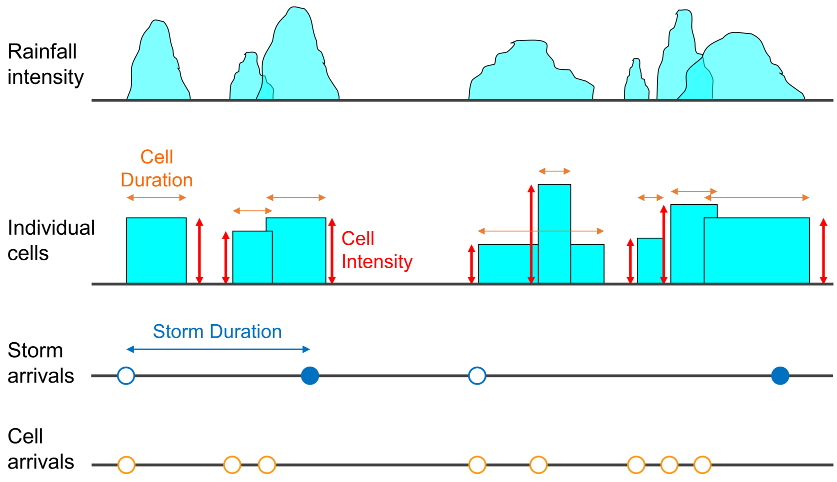

Figure 1. Illustration of the conceptualisation of the Bartlett-Lewis Rectangular Pulse model

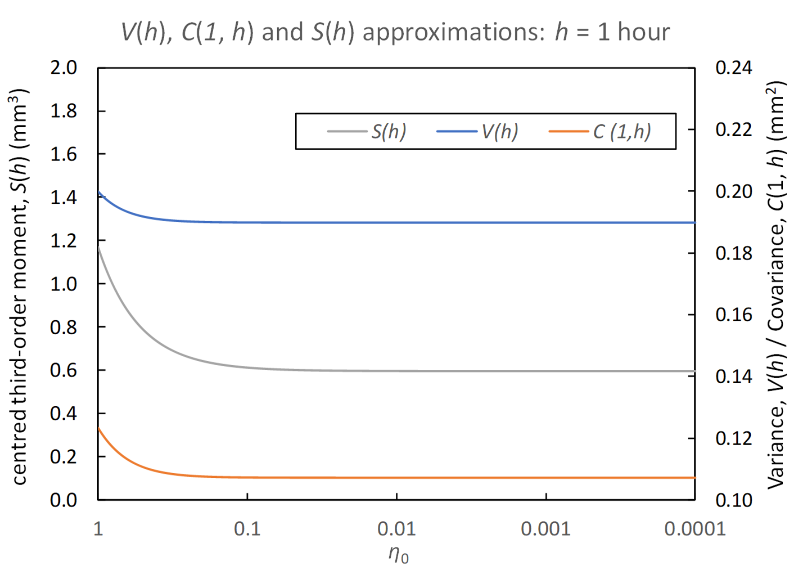

Figure 2. Changes of variance ($V(h)$), autocovaraince lag-1 ($C(1,h)$) and the third-order centred moment ($S(h)$) approximations at 1-h timescale ($h = 1$) for $\eta_0 \in (0.0001, 1)$. Parameters used are $\lambda = 0.025$, $\mu_x = 1.3$, $\alpha = 2.5$, $\nu = 0.28$, $\kappa = 0.65$ and $\phi = 0.04$.

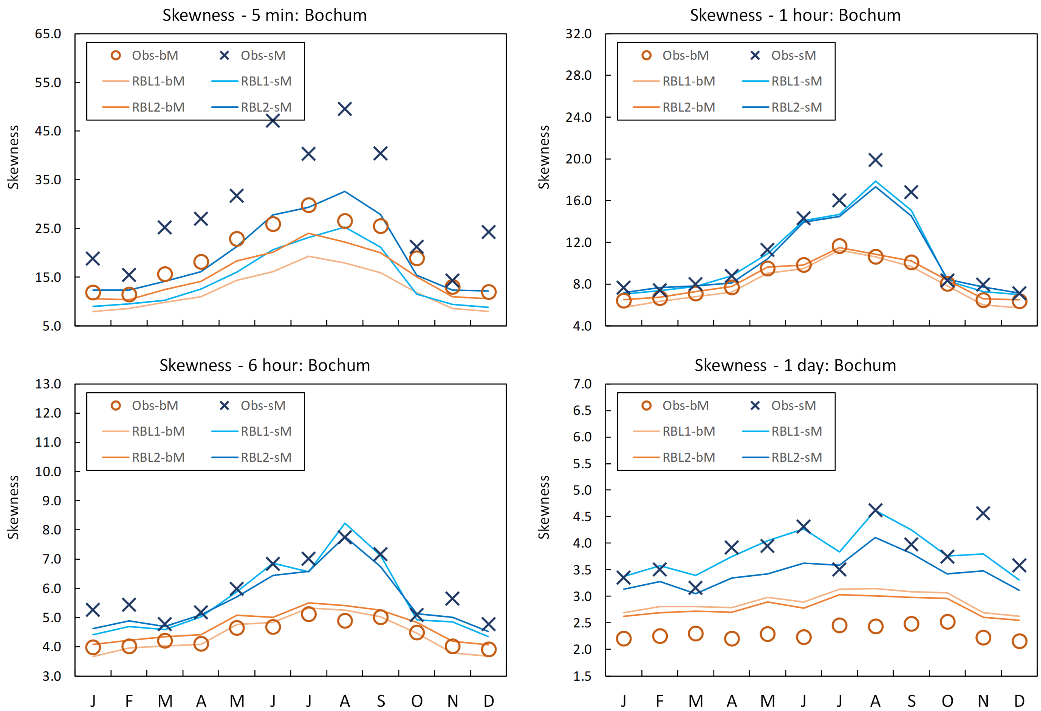

Figure 3. Coefficient of skewness by month at Bochum: the observed calculated with block (Obs-bM, orange circle markers) vs. standard (Obs-sM, blue cross markers) methods, the fitted with RBL1 (RBL1-bM, light orange line; RBL1-sM, light blue line) models, and the fitted with RBL2 (RBL2-bM, orange lines; RBL2-sM, blue lines) models

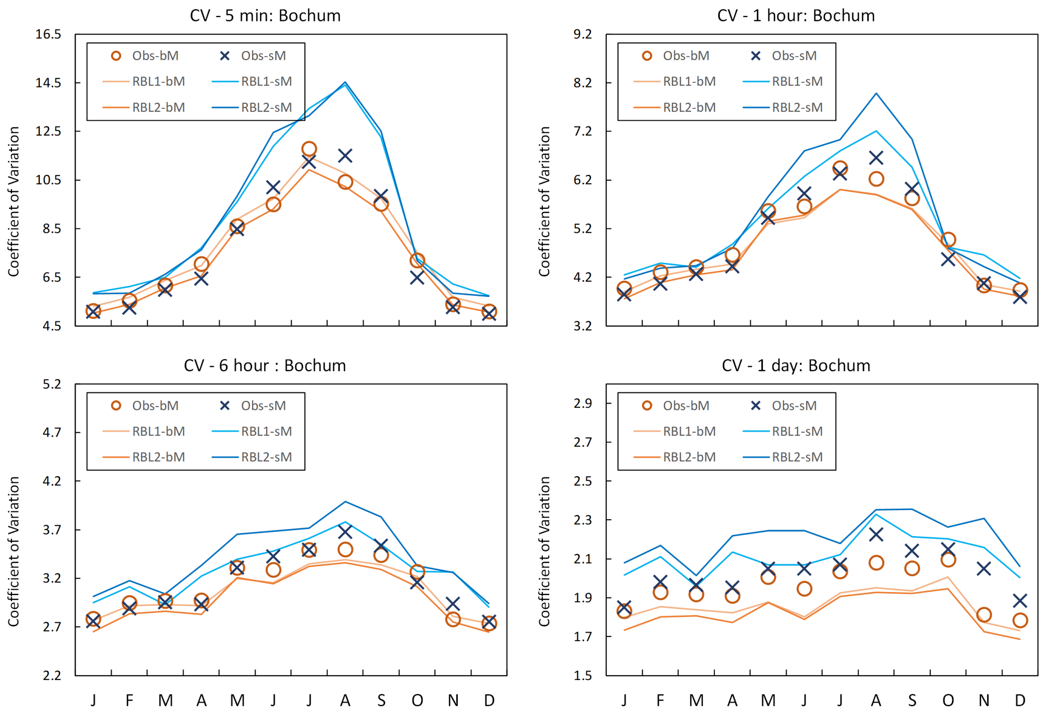

Figure 4. Coefficient of variation (CV) by month at Bochum: the observed calculated with block (Obs-bM, orange circle markers) vs. standard (Obs-sM, blue cross markers) methods, the fitted with RBL1 (RBL1-bM, light orange line; RBL1-sM, light blue line) models, and the fitted with RBL2 (RBL2-bM, orange lines; RBL2-sM, blue lines) models

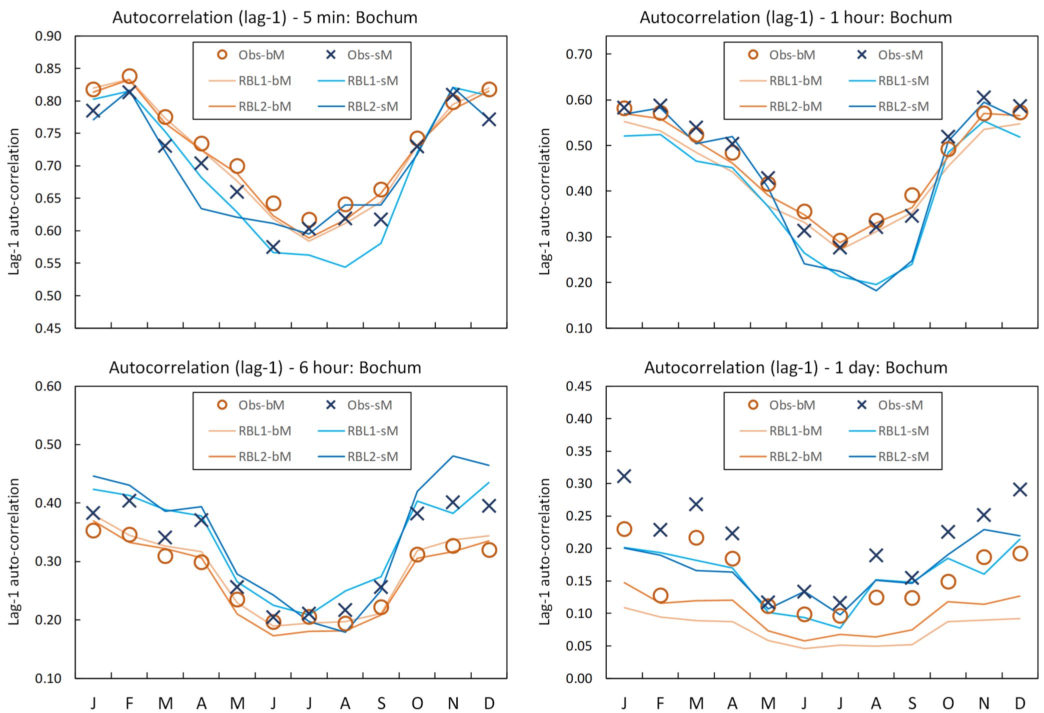

Figure 5. Autocorrelation lag-1 by month at Bochum: the observed calculated with block (Obs-bM, orange circle markers) vs. standard (Obs-sM, blue cross markers) methods, the fitted with RBL1 (RBL1-bM, light orange line; RBL1-sM, light blue line) models, and the fitted with RBL2 (RBL2-bM, orange lines; RBL2-sM, blue lines) models

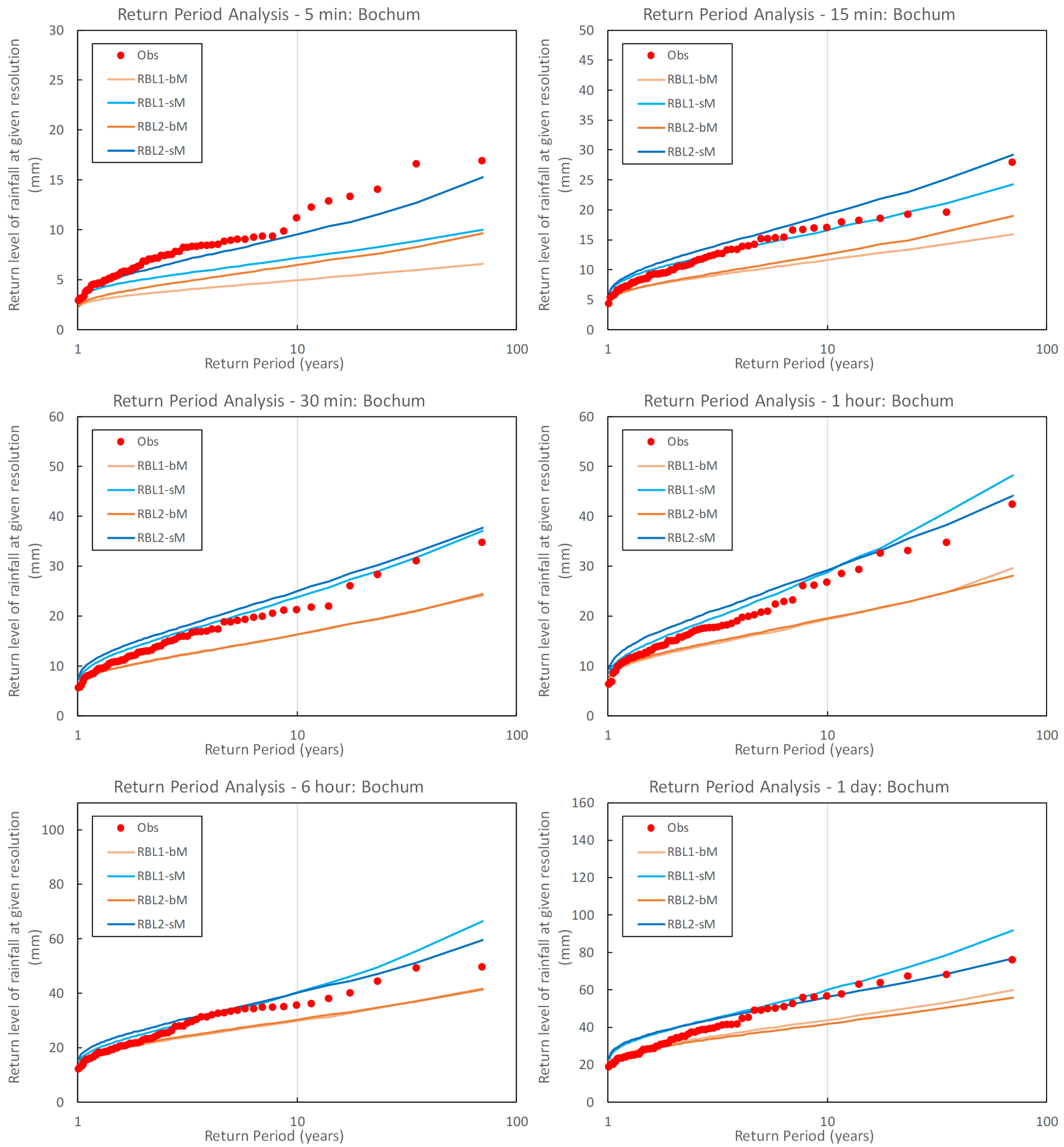

Figure 6. Observed (round markers) and simulated (lines) return levels of rainfall at different timescales at Bochum. The simulated is sampled from the RBL1 and RBL2 models fitted with selected statistical properties calculated using bM and sM methods, respectively; and the median return levels obtained from 250 simulations, each of 69 years, are illustrated.

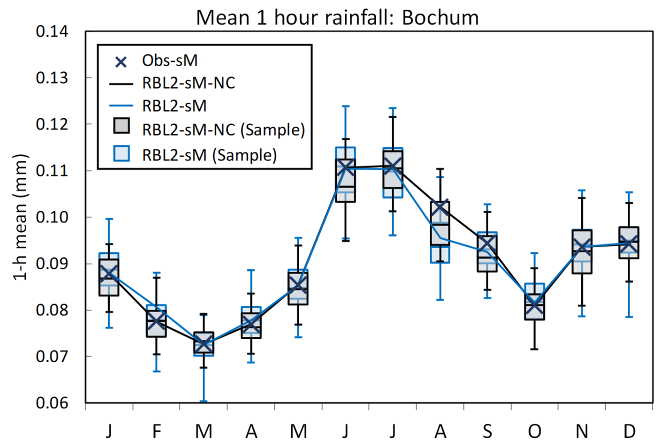

Figure 7. Mean 1-hour rainfall depths by month at Bochum: the observed vs. the fitted using RBL2 models with the original and the new solution spaces of α (RBL1-sM, light blue lines and boxplots; RBL2-sM-NC, black lines and boxplots).

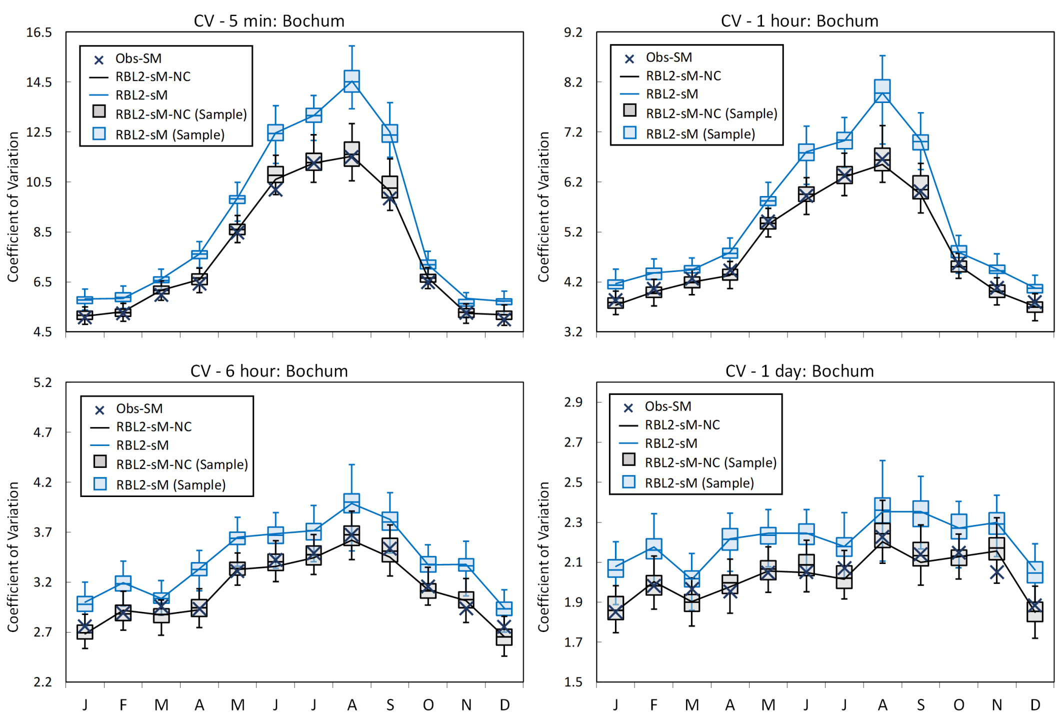

Figure 8. Coefficient of variation (CV) by month at Bochum: the observed vs. the fitted using RBL2 models with the original and the new solution spaces of α (RBL2-sM, light blue lines and boxplots; RBL2-sM-NC, black lines and boxplots).

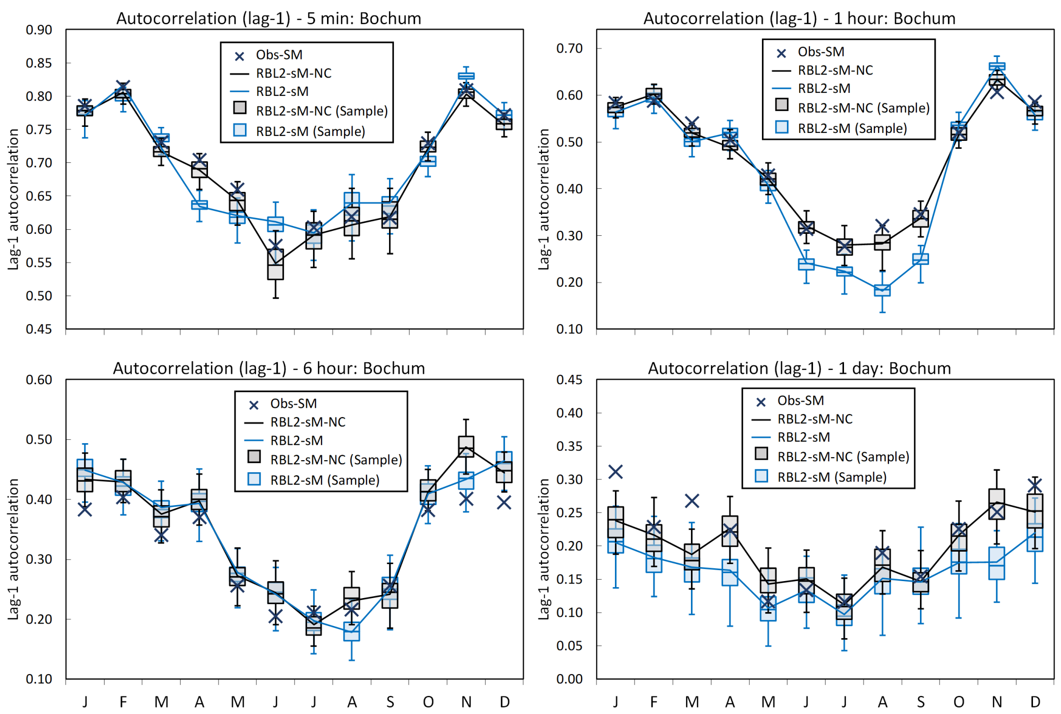

Figure 9. Autocorrelation lag-1 by month at Bochum: the observed vs. the fitted using RBL2 models with the original and the new solution spaces of α (RBL2-sM, light blue lines and boxplots; RBL2-sM-NC, black lines and boxplots).

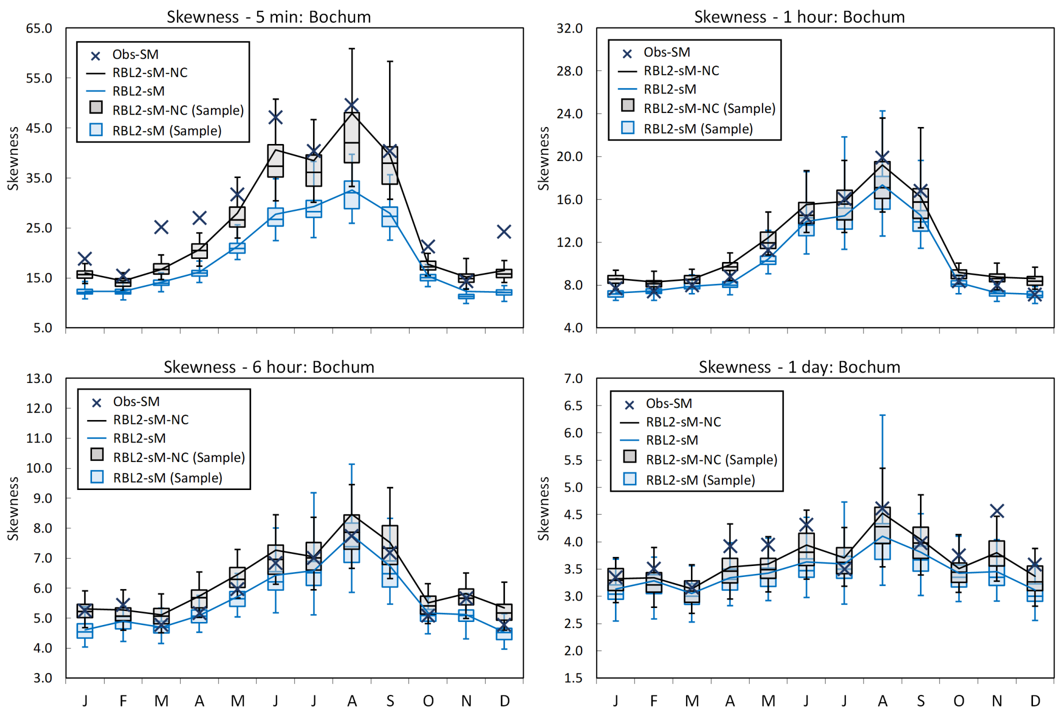

Figure 10. Coefficient of skewness by month at Bochum: the observed vs. the fitted using RBL2 models with the original and the new solution spaces of α (RBL2-sM, light blue lines and boxplots; RBL2-sM-NC, black lines and boxplots).

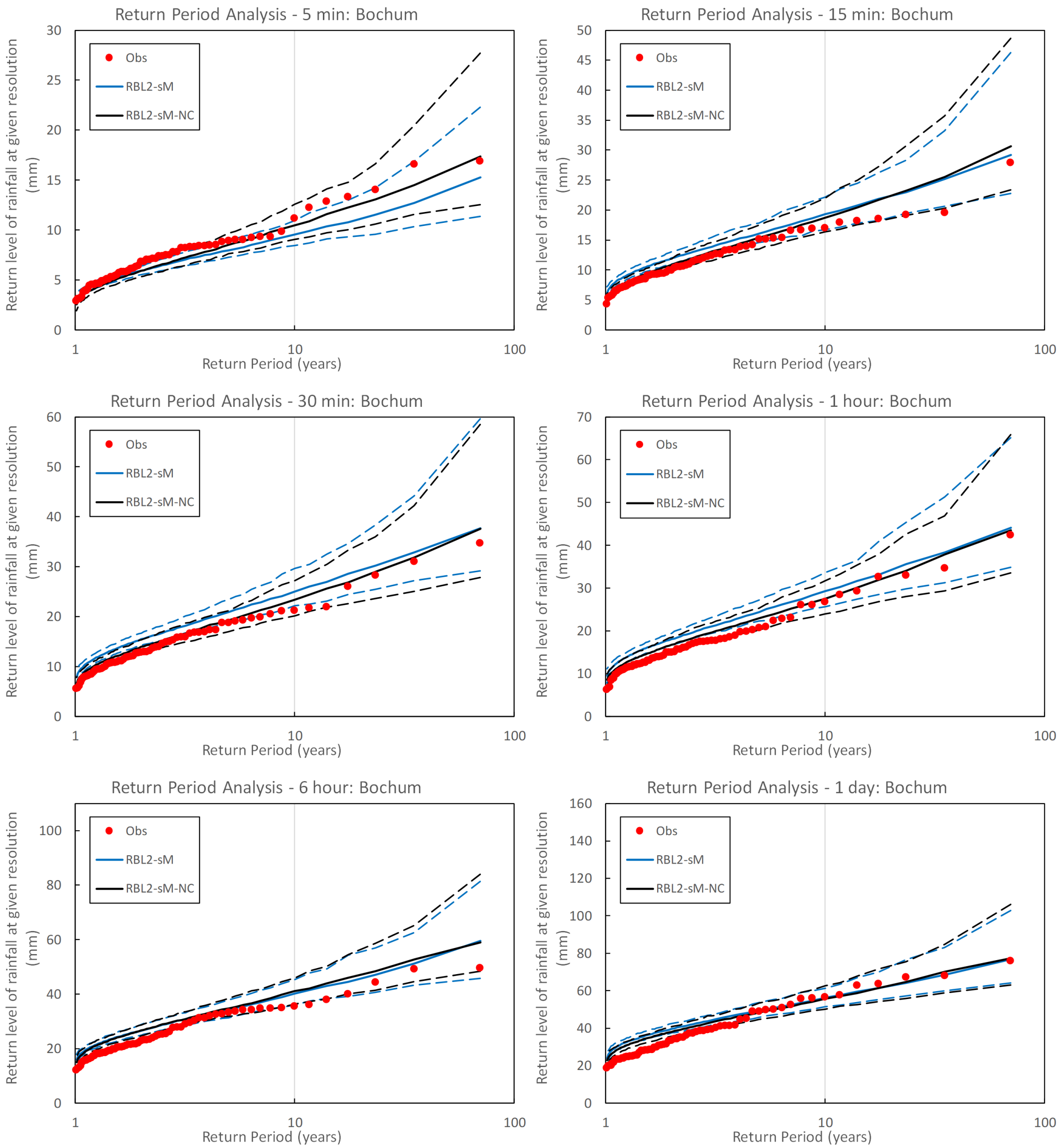

Figure 11. Observed (round markers) and simulated (lines) return levels of rainfall at multiple time-scales at Bochum. The simulated is sampled from the RBL2 models fitted with the original (blue lines) and the new (black lines) solution spaces of α. The median, 95 and 5 percentile return levels obtained from 250 simulations, each of 69 years, are plotted with solid and dashed lines, respectively.

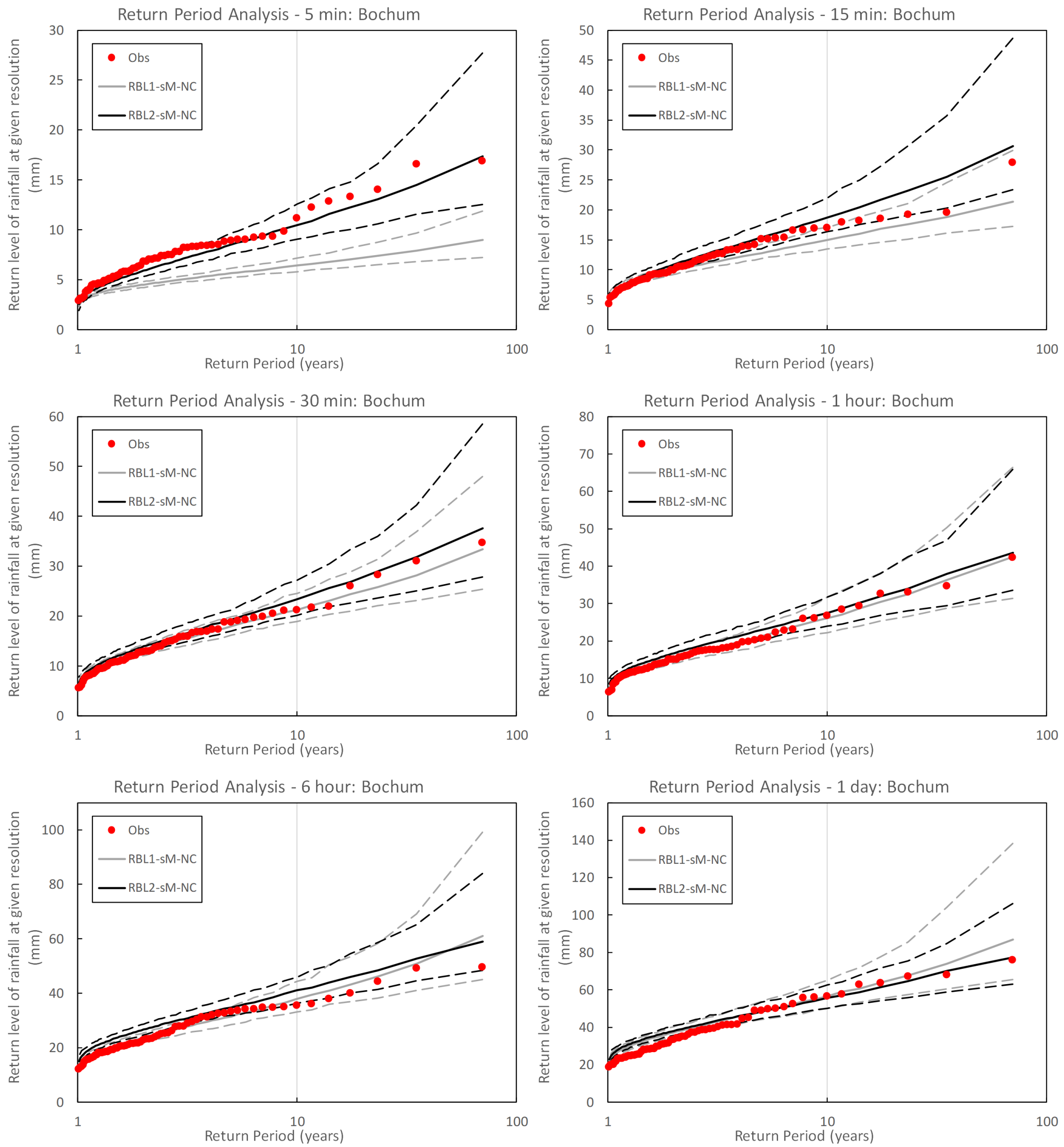

Figure 12. Observed (round markers) and simulated (lines) return levels of rainfall at multiple time-scales at Bochum. The simulated is sampled from the RBL1 (grey lines) and RBL2 (black lines) models fitted with the new solution spaces of α. The median, 95 and 5 percentile return levels obtained from 250 simulations, each of 69 years, are plotted with solid and dashed lines, respectively.

Figure 13. Daily Variances by month at Bochum: the observed calculated with standard (Obs-sM, blue cross markers) methods, the fitted with RBL1 (RBL1-bM, light orange line; RBL1-sM, light blue line; RBL1-sM-NC, grey line) models, and the fitted with RBL2 (RBL2-bM, orange lines; RBL2-sM, blue lines; RBL2-sM-NC, black line) models

Table 1. Parameters for RBL2-sM model using Bochum gauge data; constraint: $\alpha > 2$

Month	λ [h^{-1}]	ι [mm]	α [-]	α/ν [h^{-1}]	κ [-]	ϕ [-]
Jan	0.0131	0.2143	2.0000	5.9436	0.7521	0.0248
Feb	0.0124	0.2324	2.0000	4.6243	0.9185	0.0341
Mar	0.0152	0.2196	2.0000	6.9889	0.5313	0.0257
Apr	0.0125	0.2243	2.0000	11.1401	0.4508	0.0169
May	0.0143	0.4733	2.0000	10.2016	0.3166	0.0273
Jun	0.0145	1.3043	2.0000	8.3686	0.0886	0.0182
Jul	0.0173	1.3887	2.0000	8.9383	0.0818	0.0228
Aug	0.0129	1.8192	2.0000	6.9965	0.0353	0.0115
Sep	0.0127	1.2115	2.0000	7.3863	0.0918	0.0183
Oct	0.0114	0.2913	2.0000	7.1000	0.5078	0.0216
Nov	0.0100	0.2791	2.0000	4.4562	0.9070	0.0279
Dec	0.0128	0.2386	2.0019	5.6686	0.6863	0.0230

Table 2. Parameters for RBL1-sM model using Bochum gauge data; constraint: $\alpha > 4$

Month	λ [h^{-1}]	μ_X [mm h^{-1}]	α [-]	α/ν [h^{-1}]	κ [-]	ϕ [-]
Jan	0.0212	1.3041	4.0000	8.7125	0.6222	0.0318
Feb	0.0197	1.2375	4.0000	8.0948	0.6545	0.0357
Mar	0.0235	1.4790	4.0270	10.8216	0.4448	0.0279
Apr	0.0204	2.4651	4.0000	15.4629	0.3693	0.0218
May	0.0250	4.6258	4.3139	17.4875	0.2567	0.0287
Jun	0.0263	10.2162	4.4454	19.8093	0.1195	0.0227
Jul	0.0226	13.2244	7.5061	15.6796	0.0843	0.0208
Aug	0.0180	14.3142	4.5315	20.0000	0.0558	0.0111
Sep	0.0200	9.3123	4.4865	17.9124	0.0879	0.0145
Oct	0.0184	2.1201	4.0000	13.3611	0.4589	0.0232
Nov	0.0202	1.4692	4.0000	8.5970	0.8587	0.0436
Dec	0.0208	1.3561	4.0000	8.2961	0.6026	0.0305

Table 3. Parameters for RBL1-sM-NC model using Bochum gauge data; constraint: $\alpha > 2$

Month	λ	μ_X	α	α/ν	κ	ϕ
	[h^{-1}]	[mm h^{-1}]	[-]	[h^{-1}]	[-]	[-]
Jan	0.0251	1.2511	2.7887	11.4504	0.4977	0.0255
Feb	0.0227	1.1887	3.1661	9.3302	0.5924	0.0342
Mar	0.0245	1.5670	3.7514	13.4425	0.4390	0.0248
Apr	0.0252	2.0977	3.1090	18.7626	0.3714	0.0212
May	0.0250	4.6259	4.3139	17.4875	0.2567	0.0287
Jun	0.0265	9.7523	4.3302	20.0000	0.1203	0.0225
Jul	0.0226	13.2243	7.5060	15.6796	0.0843	0.0208
Aug	0.0185	8.3316	4.2836	20.0000	0.0596	0.0114
Sep	0.0200	9.3122	4.4865	17.9123	0.0879	0.0145
Oct	0.0197	2.0589	3.5292	14.6293	0.4502	0.0226
Nov	0.0274	1.3329	2.4248	12.4683	0.6338	0.0357
Dec	0.0273	1.3415	2.7193	15.3848	0.5876	0.0244

Table 4. Parameters for RBL2-sM-NC model using Bochum gauge data; constraint: $\alpha > 0$

Month	λ	ι	α	α/ν	κ	ϕ
	[h^{-1}]	[mm]	[-]	[h^{-1}]	[-]	[-]
Jan	0.0130	0.2368	0.7408	4.1819	0.7677	0.0280
Feb	0.0125	0.1985	0.9747	4.2279	1.0052	0.0333
Mar	0.0151	0.2178	0.9812	6.1830	0.5708	0.0271
Apr	0.0118	0.3137	0.7190	5.6846	0.4085	0.0206
May	0.0140	0.5276	0.6412	6.8726	0.3718	0.0353
Jun	0.0133	1.1797	0.4630	7.6713	0.1305	0.0215
Jul	0.0177	1.4427	0.6141	6.5735	0.1063	0.0318
Aug	0.0107	1.8582	0.4438	4.9260	0.0664	0.0161
Sep	0.0131	1.1473	0.4831	5.4205	0.1612	0.0306
Oct	0.0113	0.3041	1.0468	5.8242	0.5131	0.0227
Nov	0.0091	0.2344	0.8353	4.2122	1.0394	0.0243
Dec	0.0125	0.2575	0.7119	4.4430	0.6700	0.0236

Table 5. Comparison minimum objective function values for different RBL models using Bochum gauge data

Model	Jan	Feb	Mar	Apr	May	Jun	Jul	Aug	Sep	Oct	Nov	Dec
RBL1-bM	85.6	66.8	89.4	93.3	127.9	105.8	107.6	126.6	114.2	92.1	102.9	83.8
RBL2-bM	39.5	30.1	52.1	56.2	73.0	65.2	65.6	72.8	60.4	47.0	41.0	36.6
RBL1-sM	227.5	176.7	192.1	169.1	221.9	328.5	180.3	620.3	323.9	110.1	280.4	410.0
RBL2-sM	145.0	76.7	117.6	173.6	174.3	315.6	96.5	478.4	241.6	61.2	244.6	280.5
RBL1-sM-NC	186.5	169.9	192.0	149.4	221.9	328.5	180.3	620.3	323.9	107.5	104.0	348.8
RBL2-sM-NC	37.4	23.7	75.7	60.9	43.7	59.1	8.2	32.9	8.5	32.4	109.2	142.6